Sample collection and ELISA

Samples of immune sera and feces were collected every month after immunization. Sera were collected by retro-orbital puncture under anesthesia with diethyl ether and stored at −20°C. Fecal pellets (100 mg) were suspended in 0.5 ml of PBS. After centrifugation at 15,000 × *g* for 5 min, the supernatants were collected for assay. An enzyme-linked immunosorbent assay (ELISA) was performed as described elsewhere (Xin *et al.*, 2001). Briefly, 96-well microtiter plates were coated with a 10-μg/ml solution of HIV V3 region peptide (NNTRKRIQRGPGRAFVTIGKIGN; HIV V3 multiantigen peptide [MAP]) at 4°C overnight. The wells were blocked for 2 hr at room temperature with PBS containing 1% bovine serum albumin (BSA). They were then treated with 100 μl of serially diluted antiserum and incubated for an additional 1 hr at 37°C. The bound immunoglobulin was quantified with affinity-purified HRP-labeled anti-mouse antibody (Sigma, St. Louis, MO). For the estimation of fecal IgA antibody against the HIV-1, HRP-labeled goat anti-mouse IgA (Zymed Laboratories, South San Francisco, CA) was used a second antibody. The mean antibody titer was expressed as the reciprocal of the serial serum dilution that exceeded assay background by 2 SD.

Cytotoxic T lymphocyte assay

To examine antigen-specific cytotoxic T lymphocyte (CTL) activity, splenocytes were isolated 2 weeks after immunization and measured by standard 6-hr ^{51}Cr release assay mediated by lysis of P815 (*H-2*^{d}) cells as previously described (Xin *et al.*, 2001). Briefly, 1×10^6 splenocytes per well were restimulated for 5 days in a 24-well plate with a 10-μg/ml concentration of HIV-1 V3 peptide (RGPGRAFVTI, MHC class I restricted). Approximately 1×10^6 P815 cells were pulsed *in vitro* with HIV-1 V3 peptide (10 μg/ml) for 2 hr. These P815 cells were labeled with ^{51}Cr for 90 min, lethally irradiated at 30 Gy, and used as target cells. The ratios of effector cells to target cells were 5:1, 20:1, and 80:1. The percentage of specific ^{51}Cr release was calculated as [(experimental release − spontaneous release)/(maximum release − spontaneous release)] × 100. Target cells incubated in medium alone and with medium plus 5% Triton X-100 were used to determine spontaneous and maximum chromium release, respectively.

Interferon γ ELISpot assay and computer-assisted video image analysis

Interferon γ (IFN-γ) enzyme-linked immunospot (ELISpot) assays were performed 2 weeks after immunization as previously described (Xin *et al.*, 2002). Intestinal lymphocytes were isolated from Peyer's patches, lamina propria, and intestinal lymph nodes. Briefly, a MultiScreen-IP plate (Millipore) was coated with 50 μl of purified rat anti-mouse IFN-γ antibody (XMG1.2, 10 μg/ml; BD Biosciences Pharmingen, San Diego, CA) in PBS overnight at 4°C. The wells of the plate were then blocked with PBS–5% BSA and 0.025% Tween 20 for 2 hr at room temperature. Lymphocytes ($1–10 \times 10^5$) isolated from spleen or intestinal lymphocytes were added to the wells, in triplicate. To examine HIV-specific CTL activity, spleen cells were stimulated for 24 hr at 37°C with HIV V3 peptide (NNTRKRIQRGPGRAFVTIGKIGN) at 10 μg/ml. Control wells contained sperm whale myoglobin peptide (ALVEADVA). After incubation, cells were removed and incubated with biotinylated anti-mouse IFN-γ antibody (0.5 μg/ml; BD Biosciences Pharmingen) for 2 hr at 37°C, followed by adding 0.2% alkaline phosphatase–streptavidin (100 μl/well; Vector Laboratories, Burlingame, CA) in PBS containing 0.05% Tween 20 and 5% BSA for 1.5 hr. Finally, the plate was treated with 5-bromo-4-chloro-3-indolyl phosphate/nitroblue tetrazolium (BCIP/NBT)–membrane phosphatase (50 μl/well; Kirkegaard & Perry Laboratories, Gaithersburg, MD) at room temperature for 20 min and the reaction was stopped under running distilled water. Numbers of spots were automatically determined by computer-assisted video image analysis (Herr *et al.*, 1997).

Tetramer assay

The tetramer assay was carried out 2 weeks after immunization. The H-2D/p18 tetramer (RGPGRAFVTI) labeled with phycoerythrin (PE) was prepared by the NIH AIDS Research and Reference Reagent Program. The tetramer assay is described elsewhere (Altman *et al.*, 1996; Villacres *et al.*, 2000). Briefly, mouse splenocytes were incubated for 30 min at 4°C with 4% normal mouse serum in PBS. Cells were stained with fluorescein isothiocyanate (FITC)-labeled anti-mouse CD8a (Ly-2; BD Biosciences Pharmingen) at 0.5 μg/10^6 cells for 30 min at 4°C. After two washes in staining buffer (3% fetal calf serum [FCS], 0.1% NaN_3 in PBS), the cells were incubated with the tetramer reagent for 15 min at 37°C followed by flow cytometric analysis. In some experiments, the splenocytes were stimulated for 3 days with HIV V3 peptide (NNTRKRIQRGPGRAFVTIGKIGN) or sperm whale myoglobin peptide at 10 μg/ml before being stained with CD8a antibody and the tetramer reagent.

Recombinant vaccinia virus used for challenge studies

The virus challenge experiment was performed 2 weeks after immunization as described previously (Belyakov *et al.*, 1998). Recombinant vaccinia virus vPE16 expressing HIV-1 *env* gene (Cat. No. 362; NIH AIDS Research and Reference Reagent Program) was used for the study. Briefly, 2 weeks after immunization, mice were challenged intrarectally with 2.5×10^7 plaque-forming units (PFU) of vaccinia virus vPE16. Six days after the challenge with recombinant vaccinia virus the mice were sacrificed and their ovaries were removed, homogenized, sonicated, and assayed for vPE16 titer by applying serial 10-fold dilutions to a plate of CV1 cells, staining with crystal violet, and counting plaques at each dilution.

Induction of HIV-specific IFN-γ-secreting CD8$^+$ T cells by AAV-HIV-infected dendritic cells

Dendritic cells (DCs) were isolated from BALB/c mouse bone marrow as previously described (Behboudi *et al.*, 2000). Briefly, bone marrow was removed from the tibia and femur of BALB/c mice. Bone marrow cells (5×10^5/ml) were cultured in RPMI 1640 containing 10% FCS and recombinant granulocyte-macrophage colony-stimulating factor (rGM-CSF, 1 ng/ml; KiRin Beer, Tokyo, Japan) plus recombinant interleukin 4 (rIL-4) for 6 days. CD11c$^+$ DCs were purified with CD11c (N418) mi-

crobeads (Miltenyi Biotech, Auburn, CA) according to the manufacturer instructions. The $CD11c^+$ DCs were infected with AAV-LacZ at 10^4 particles/cell at 37°C for 1 hr. The cells were then washed, and 5×10^6 cells were adoptively transferred into the tail vein of recipient BALB/c mice. One week after administration, the number of HIV-specific IFN-γ-secreting splenocytes was measured by the intracellular cytokine staining (ICCS) method.

Intracellular cytokine staining

The ICCS assay was performed according to the instructions of the Cytofix/Cytoperm Plus kit manufacturer (BD Biosciences Pharmingen). Briefly, splenocytes were stimulated for 24 hr with a 10-μg/ml concentration of the HIV V3 peptide (NNTRKRIQRGPGRAFVTIGKIGN). GolgiPlug (1 μl/ml; BD Biosciences Pharmingen) was added for the last 2 hr of stimulation. Cells were washed with staining buffer (3% FCS, 0.1% NaN_3 in PBS), blocked with 4% normal mouse serum, and stained with PE-labeled anti-mouse CD8a antibody (Ly-2; BD Biosciences Pharmingen). The cells were then suspended in 250 μl of Cytofix/Cytoperm solution at 4°C for 20 min, washed with Perm/Wash solution, and stained with FITC-labeled anti-mouse IFN-γ antibody (BD Biosciences Pharmingen) at 4°C for 30 min followed by flow cytometric analysis.

Data analysis

All values are expressed as means ± SE. Statistical analysis of the experimental data and controls was conducted by one-way factorial analysis of variance. Significance was defined as $p < 0.05$ in these statistical analyses.

RESULTS

Detection of HIV expression

HIV mRNA was detectable in small intestine on days 1, 3, 7, and 14 after oral administration of AAV-HIV vector, and in draining lymph nodes on days 1, 3, and 7, but not in spleen at any of the four time points (Fig. 1).

AAV-HIV immunization stimulates a humoral immune response

BALB/c mice were immunized with 10^8–10^{11} AAV-HIV particles. The resultant HIV-specific serum antibody response was examined 2 months later. Anti-HIV IgG antibody titers rose as a function of immunization dose, with 10^{10}–10^{11} AAV-HIV particles inducing the greatest immunity (Fig. 2A). The time course of this response was monitored in mice immunized with 10^{10} particles of AAV-HIV. The highest titers of serum IgG and fecal IgA were observed 2 months after immunization, reaching background levels by 6 and 4 months, respectively (Fig. 2B and C).

AAV-HIV immunization stimulates a cellular immune response

Three assays were used to monitor the induction of a cellular immune response after immunization with 10^{10} AAV-HIV particles. In a CTL assay measuring the lysis of HIV V3 peptide-pulsed targets, spleen cells from immunized animals specifically killed target cells at an effector:target ratio as low as 5:1, but not the spleen cells from AAV-LacZ vector-administered

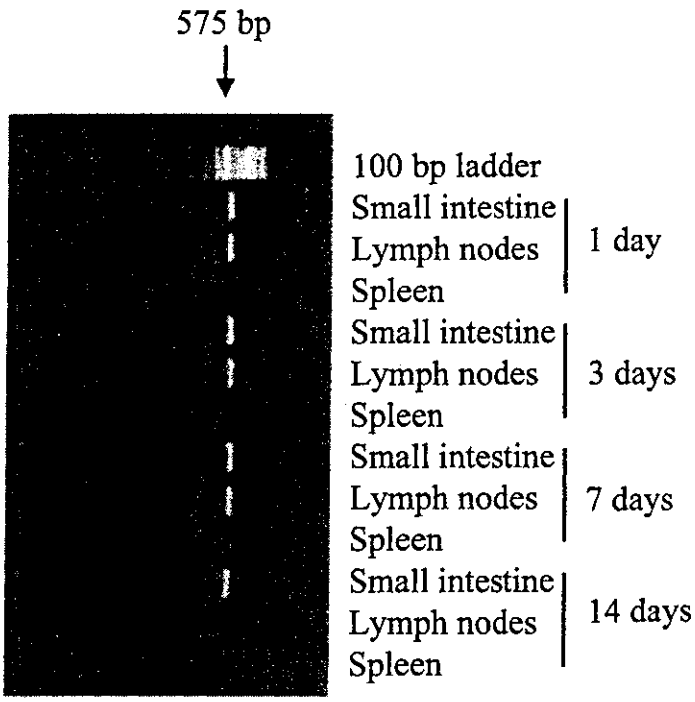

FIG. 1. Detection of HIV mRNA by RT-PCR. On days 1, 3, 7, and 14 after oral administration of 10^{10} particles of AAV-HIV vector, HIV mRNA in small intestinal tissue, intestinal draining lymph nodes, and spleen was detected by reverse transcriptase-polymerase chain reaction (RT-PCR). The RT-PCR product was analyzed on a 2% agarose gel.

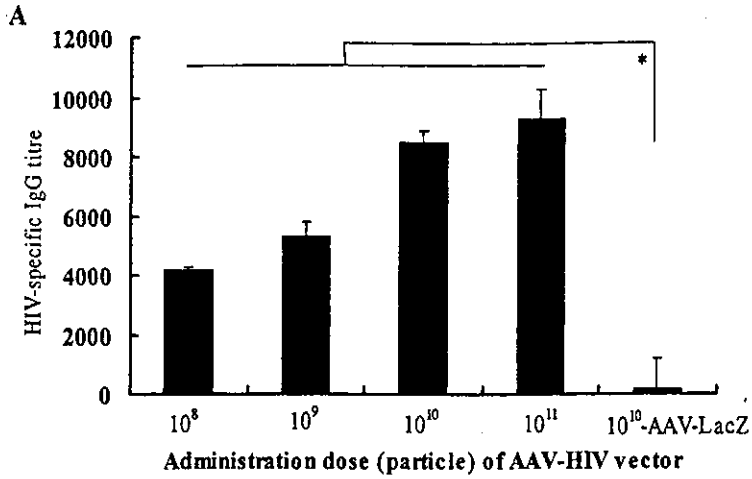

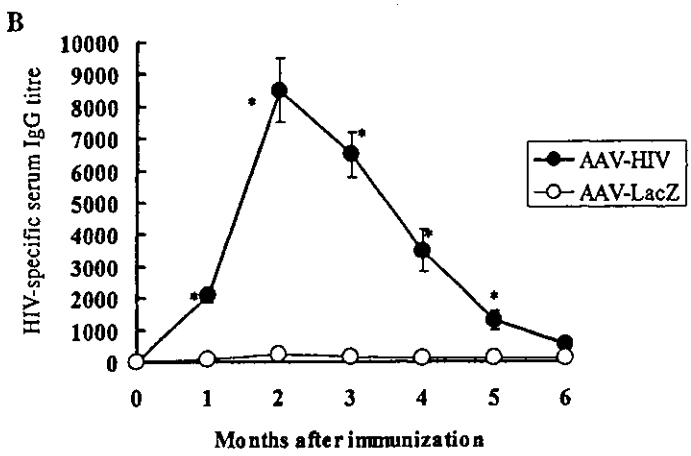

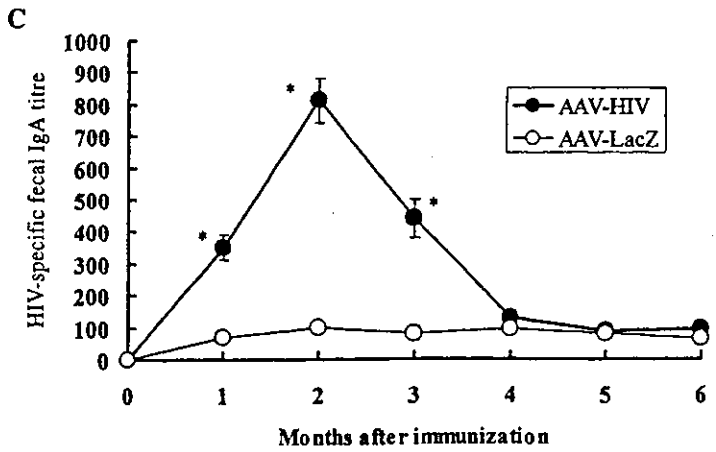

FIG. 2. HIV-specific serum IgG and fecal IgA titers induced by oral administration of AAV-HIV vector. (A) HIV-specific serum IgG titer. Serum from BALB/c mice 2 months postimmunization was studied by ELISA. (B and C) Time course of humoral immune response elicited by AAV-HIV vector: (B) HIV-specific serum IgG titer and (C) HIV-specific fecal IgA titer. AAV-HIV particles (10^{10}) were administered orally to mice. Blood and feces were collected monthly and HIV-specific antibody titers were determined by ELISA. Data represent the average of five mice per group. *Mean values significantly different from animals treated with 10^{10} AAV-LacZ.

animals (Fig. 3). Consistent with this finding, there was a significant increase in the number of lymphocytes in the spleen and intestine of immunized mice that secreted IFN-γ when stimulated with V3 peptide *in vitro* compared with AAV-LacZ treated animals (Fig. 4). Furthermore, the number of IFN-γ-secreting lymphocytes isolated from intestine was significantly higher than that from spleen in the AAV-HIV immunized mice.

A tetramer binding assay was used to identify MHC class I-restricted HIV-specific T cells present in immunized mice (Altman *et al.*, 1996). Whereas 0.04% of $CD8^+$ splenocytes from control mice bound HIV peptide p18, 0.6% of the $CD8^+$ splenocytes from AAV-HIV-immunized mice showed this specificity 2 weeks after oral immunization. When these cells were restimulated *in vitro* for 3 days, this Ag-specific population expanded to constitute 12.6% of the $CD8^+$ splenocytes (Fig. 5). To examine whether oral administration of AAV-HIV particles induced a protective immune response, vaccinated mice were challenged with vaccinia virus vPE16, which expresses the HIV *env* gene. As shown in Fig. 6, oral administration of AAV-HIV vaccine reduced viral load by >30-fold ($p < 0.05$).

DCs present HIV peptide to T cells in vivo

To examine whether DCs play a role in AAV-HIV-induced immune responses, DCs were purified from the bone marrow of unimmunized mice. DCs were then treated with AAV-HIV particles and administered intravenously to normal mice. Seven days after DC administration, the frequency of HIV-specific IFN-γ-secreting splenocytes was measured by ICCS assay. Recipients of the AAV-HIV-transfected cells had 4-fold more cytokine-secreting $CD8^+$ T cells than did AAV-LacZ-treated control (Fig. 7, top). When these cells were restimulated with the HIV V3 peptide *in vitro*, a further 12-fold increase in HIV-specific T cells was obtained (Fig. 7, bottom). However, the frequency of HIV-specific IFN-γ-secreting splenocytes was not detectable by ICCS assay when using whale myoglobin peptide as a stimulator (0.02 and 0.08% for AAV-LacZ vector- and AAV-HIV vector-administered mice, respectively; data not shown). These data demonstrate that AAV-HIV-infected DCs can induce HIV-specific CTL responses *in vivo*, and suggest that such cells play an important role in AAV-HIV vaccine-induced immune responses.

DISCUSSION

This study demonstrates that oral administration of AAV-HIV induces systemic and regional immune responses that provide a degree of protection against mucosal infection. These results are consistent with previous work demonstrating that genes encoding foreign pathogens and transfected into host cells via AAV vectors generate cellular and humoral immune responses against the encoded antigen (Manning *et al.*, 1997; During *et al.*, 1998; Brockstedt *et al.*, 1999; Sarukhan *et al.*, 2001; Xin *et al.*, 2001). However, the majority of such reports examined the durability of transgene expression after intramuscular administration of the AAV vector, a strategy that did not typically induce a strong cell-mediated immune response against the transgene (Flotte *et al.*, 1993; Xiao and Samulski, 1996; Fisher *et al.*, 1997). Unlike studies in which the encoded protein was syngeneic (as in gene therapy) or in which a neoantigen was used to evaluate long-term expression (such as β-galactosidase), the immune response elicited by our HIV *env*-encoding vector was strong.

Ease of distribution and administration favors the development of oral vaccines. Orally administered antigens are scavenged by intestinal M cells and rapidly taken up by antigen-presenting cells (APCs) in Peyer's patches and the lamina propria. Oral vaccines can induce three forms of immunity: cell mediated, humoral, and mucosal immunity (Eriksson *et al.*, 1993; Lewis *et al.*, 1994). This triad can be extremely important in protecting the host from infectious diseases, such as AIDS. In this study, oral immunization with AAV-HIV induced both systemic humoral and CMI responses (Figs. 2, 3, and 5) and mucosal CMI (Fig. 4), consistent with results from During *et al.* (2000). Of particular importance, the immunity induced

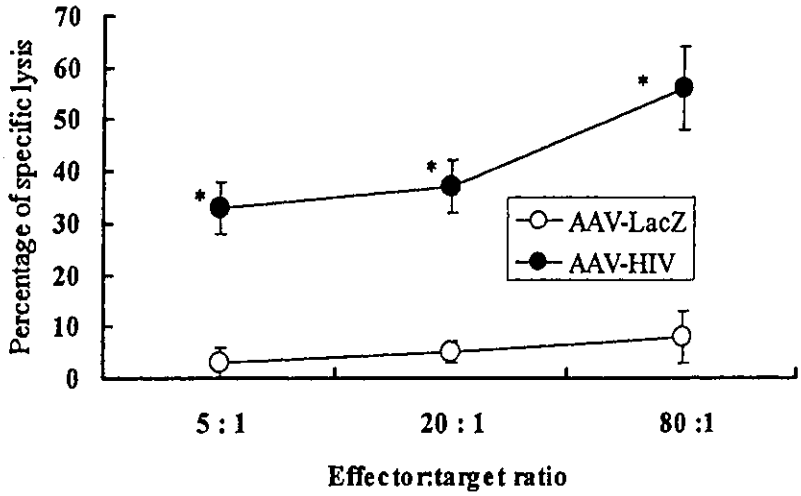

FIG. 3. CTL response of mice orally administered 10^{10} AAV-HIV particles. Spleen cells from mice immunized 2 weeks earlier were expanded *in vitro* for 5 days in the presence of V3 peptide. Cytotoxicity was evaluated with V3 peptide-pulsed target cells. Data represent the averaged of three mice per group. *Mean values significantly different from the group treated with AAV-lacZ.

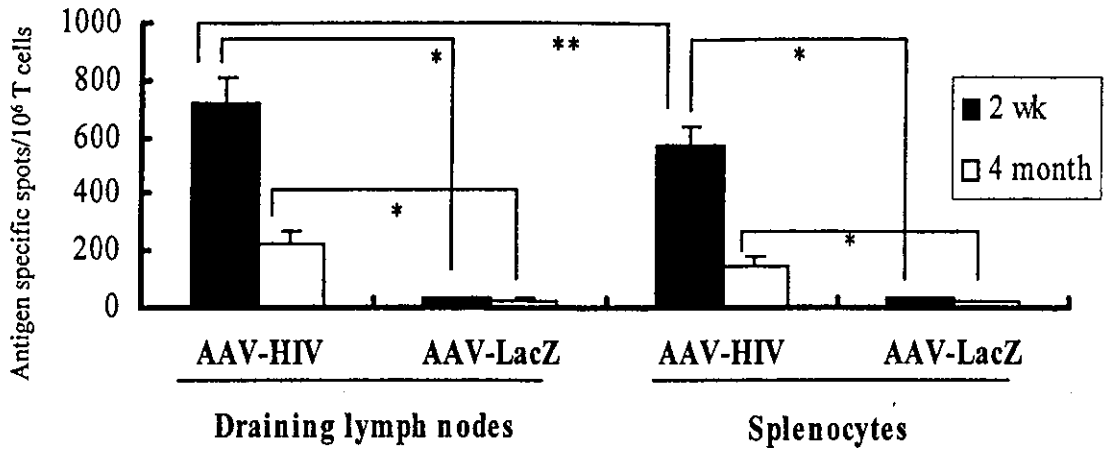

FIG. 4. IFN-γ response of mice orally administered 10^{10} AAV-HIV particles. Spleen and intestinal lymphocytes were isolated from mice immunized 2 weeks earlier, and stimulated to secret IFN-γ by incubation with V3 peptide. The number of IFN-γ-secreting cells was determined by ELISpot assay. Data represent the average of four mice per group. *Mean values significantly different between groups administered AAV-HIV and AAV-LacZ. **Mean values significantly different between intestinal lymphocytes and splenocytes.

by orally administered AAV-HIV significantly reduced the viral load of animals challenged with HIV *env*-expressing vaccinia virus after intrarectal challenge (Fig. 6). These results suggest that with further development, oral administration of AAV-HIV may provide an effective means of HIV vaccination. Compared with other viral vectors, AAV vector has considerable advantages in physical and chemical characteristics for oral administration. For example, AAV is stable at high temperatures (56°C for 1 hr) and a wide range of pH, and is resistant to proteinase digestion (Ozawa, 1997).

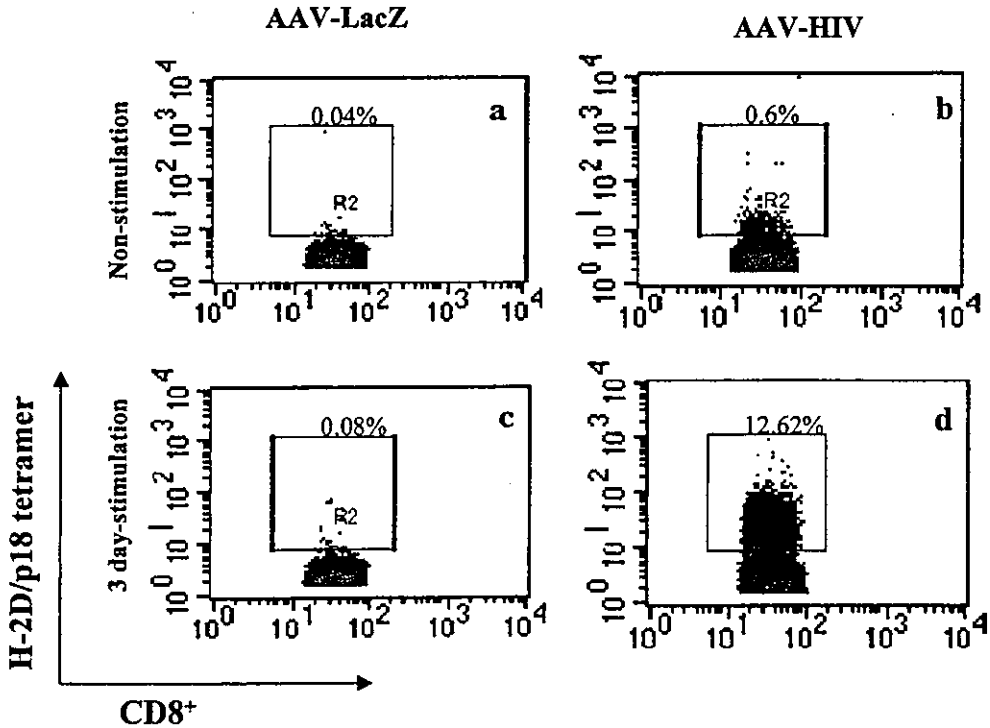

FIG. 5. Frequency of HIV-specific CD8$^+$ spleen cells in mice orally administered 10^{10} AAV-HIV particles. The number of CD8$^+$ spleen cells expressing TCR that recognized the MHC class I-restricted p18 tetramer from HIVgp160 was examined 2 weeks postimmunization. (a and b) Binding of the H-2D/p18 tetramer to freshly isolated CD8$^+$ T cells from AAV-lacZ- and AAV-HIV-immunized mice, respectively. (c and d) Binding of the H-2D/p18 tetramer to CD8$^+$ T cells that were restimulated *in vitro* by V3 peptide for 3 days. Similar results were obtained in two other independent experiments.

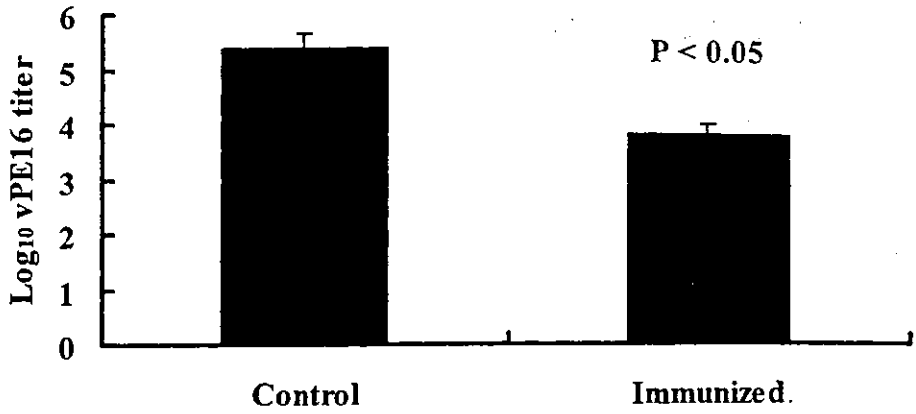

FIG. 6. Resistance of immunized mice to infection with vaccinia virus (vPE16) expressing the HIV *env* gene. Mice were orally administered 10^{10} particles of AAV-HIV or AAV-LacZ. Two weeks later, they were challenged intrarectally with 10^7 PFU of vPE16 virus. Vaccinia virus titers were measured 6 days after virus challenge. Data represent the average of 10 mice per group.

DCs are primarily responsible for stimulating resting naive T lymphocytes and initiating a CTL response (Banchereau and Steinman, 1998). Immature DCs residing in peripheral tissues capture foreign antigens, and then mature and migrate to secondary lymphoid organs, where the processed antigen is presented. To determine whether DCs contributed to the immune responses induced by oral AAV-HIV, purified $CD11c^+$ DCs were infected with AAV-LacZ. Results show that β-galactosidase was strongly expressed by transfected DCs for at least 7 days (data not shown). In addition, we found that transfection

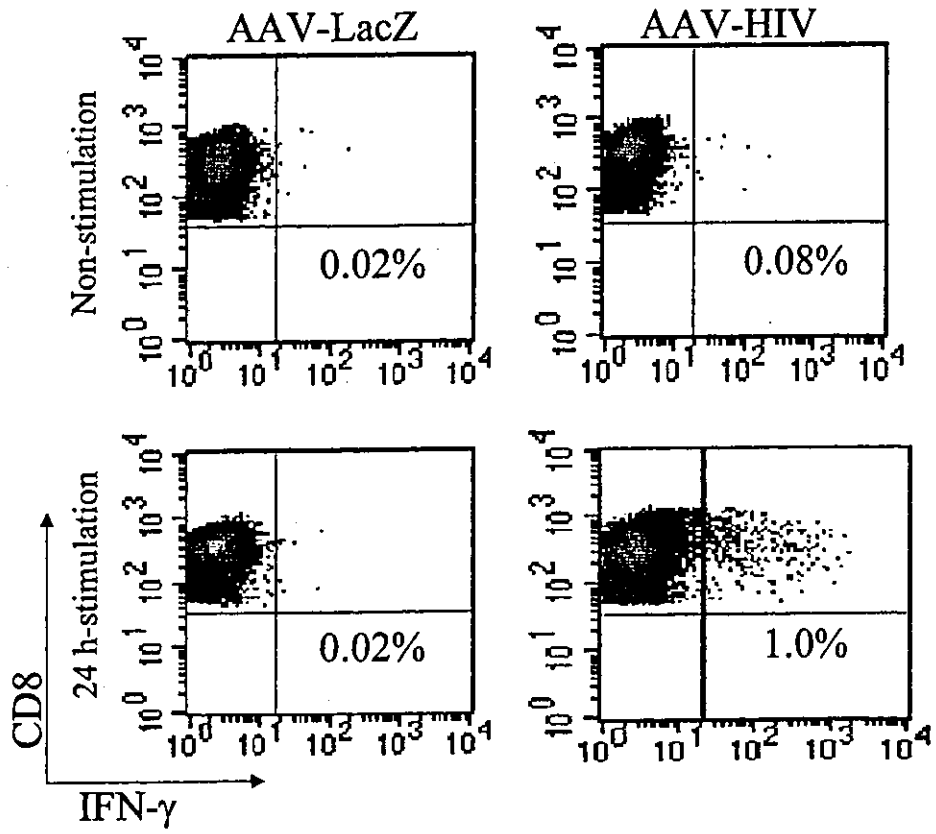

FIG. 7. Induction of an HIV-1-specific CTL response *in vivo* by transfer of AAV-HIV-transfected DCs. AAV-HIV or AAV-lacZ (10^4 particles) was used to infect bone marrow-derived DCs *in vitro*. The cells were washed, and injected intravenously into naive recipient BALB/c mice. One week later, splenocytes were isolated and stimulated with V3 peptide for 24 hr. IFN-γ-secreting $CD8^+$ splenocytes were detected by ICCS assay. Similar results were obtained in two additional independent experiments.

with an AAV vector promoted the maturation of bone marrow-derived immature DCs (data not shown). Consistent with DCs playing a role in anti-HIV immunity, DCs transfected with AAV-HIV and transferred into naive mice induced the generation of HIV-specific IFN-γ secretion by $CD8^+$ T cells (Fig. 7). These results demonstrate that DCs can present vector-encoded antigen to naive T cells. These findings are consistent with those of Zhang *et al.* (2000), but contrast with those of Sarukhan *et al.* (2001). Ponnazhagan *et al.* showed that AAV vector can be efficiently transduced into human peripheral blood monocytes and monocyte-derived DCs and supported the utility of AAV vectors for future human DC vaccine studies (Ponnazhagan *et al.*, 1997, 2001). However, our results suggest that AAV-LacZ-infected DCs strongly expressed LacZ protein, and that the infection efficiency of AAV-2-based vector into mouse bone marrow DCs was low (1–5% DCs were infected with AAV-LacZ at 10^4 particles per DC; data not shown). Those differences may be due to different species and different doses in those experiments.

In this study, oral immunization with AAV-HIV vector induced mucosal, humoral, and cell-mediated responses. We propose that there are three potential pathways responsible for antigen presentation after oral administration of AAV vector: (1) AAV vector infects epithelium and muscle cells of intestine and stomach. The cells express the encoded protein antigen and present it to immune cells; (2) AAV vector infects epithelium and muscle cells of intestine and stomach. The cells express the encoded protein antigen, with the antigen then being transmitted to APCs; or (3) AAV vector directly infects APCs, which express the encoded protein and present it to T and B cells. When we orally administered AAV-LacZ vector or AAV-HIV vector, more epithelium of intestine and stomach was stained with X-Gal than muscle cells of intestine and stomach, and HIV mRNA was detected in the tissue of small intestine (Fig. 1). These data support the first and second proposals. The data can also be explained as a rapid decline in antibody titer (Fig. 2B and C); generally, the epithelial cells of the small intestine are known to be renewed in 2–3 days (Cheng and Leblond, 1974). The detectable HIV mRNA in the small intestine lymph nodes and our *ex vivo* results (Fig. 7) suggest the importance of the third proposal in oral vaccine-induced immune responses.

A 23-mer HIV peptide was used in place of the 10-mer HIV peptide as a stimulant in the ELISpot assay, ICCS assay, and tetramer assay (see Materials and Methods). Our previous experiments suggested that a 10-mer HIV peptide could stimulate the immune system sufficiently; however, the 23-mer HIV peptide was more sensitive than the 10-mer peptide in the three assays. Because a full-length HIV *env* gene was expressed by the AAV-HIV vector, we used the 23-mer HIV peptide in these assays.

Although this work evaluated the effect of administering AAV-HIV only once, we are currently examining the effect of booster immunizations. Preliminary results suggest that primary exposure to the vector induces a strong AAV-specific immune response that blunts the effect of subsequent vaccinations (Chirmule *et al.*, 2000; Halbert *et al.*, 2000). Further studies evaluating the use of AAV-HIV in combination with other HIV immunogens (such as recombinant protein or DNA vaccines) in a prime–boost strategy are planned. Findings to date indicate that oral administration of AAV-HIV induces strong humoral and cellular immune responses that significantly reduce the viral load of animals intrarectally challenged with HIV *env*-expressing vaccinia virus.

ACKNOWLEDGMENTS

We are grateful to Ms. M. Kawano for technical assistance and to Ms. T. Takeishi and A. De La Fuente for secretarial assistance. We also extend our appreciation to Avigen (Alameda, CA) for supplying the AAV plasmids in this study. This work was partially supported by a Grant-in-Aid from the Ministry of Education, Science, Sports, and Culture of Japan, by the Ministry of Health and Welfare of Jápan, and by the Japan Health Sciences Foundation (K-1027).

REFERENCES

ALDOVINI, A., and YOUNG, R.A. (1991). Humoral and cell-mediated immune response to live recombinant BCG-HIV vaccines. Nature **351,** 479–482.

ALTMAN, J.D., MOSS, P.A.H., GOULDER, P.J.R., BAROUCH, D.H., MCHEYZER-WILLIAMS, M.G., BELL, J.I., MCMICHAEL, A.J., and DAVIS, M.M. (1996). Phenotypic analysis of antigen-specific T lymphocytes. Science **274,** 94–96.

BANCHEREAU, J., and STEINMAN, R.M. (1998). Dendritic cells and the control of immunity. Nature **392,** 245–252.

BEHBOUDI, S., CHAO, D., KLENERMAN, P., and AUSTYN, J. (2000). The effects of DNA containing CpG motif on dendritic cells. Immunology **99,** 361–366.

BELSHE, R.B., GORSE, G.J., MULLIGAN, M.J., EVANS, T.G., KEEFER, M.C., EXCLER, J.L., DULIEGE, A.M., TARTAGLIA, J., COX, W.I., MCNAMARA, J., HWANG, K.L., BRADNEY, A., MONTEFIORI, D., and WEINHOLD, K.J. (1998). Induction of immune responses to HIV-1 by canarypox virus (ALVAC) HIV- and gp120 SF-2 recombinant vaccines in uninfected volunteers. AIDS **12,** 2407–2415.

BELYAKOV, I.M., DERBY, M.A., AHLERS, J.D., KELSALL, B.L., EARL, P., MOSS, B., STROBER, W., and BERZOFSKY, J.A. (1998). Mucosal immunization with HIV-1 peptide vaccine induces mucosal and systemic cytotoxic T lymphocytes and protective immunity in mice against intrarectal recombinant HIV–vaccinia challenge. Proc. Natl. Acad. Sci. U.S.A. **95,** 1709–1714.

BROCKSTEDT, D.G., PODSAKFF, G.M., FONG, L., KURTZMAN, G., MUELLER-RUCHHOLTZ, W., and ENGLEMAN, E.G. (1999). Induction of immunity to antigens expressed by recombinant adeno-associated virus depends on the route of administration. Clin. Immunol. **92,** 67–75.

CALEY, I.J., BETTS, M.R., DAVIS, N.L., SWANSTROM, R., FRELINGER, J.A., and JOHNSTON, R.E. (1999). Venezuelan equine encephalitis virus vectors expressing HIV-1 proteins: Vector design strategies for improved vaccine efficacy. Vaccine **17,** 3124–3135.

CHENG, H., and LEBLOND, C.P. (1974). Origin, differentiation and renewal of the four main epithelial cell types in the mouse small intestine. Am. J. Anat. **141,** 461–480.

CHIRMULE, N., ZIAO, W., TRUNEH, A., SCHNELL, M.A., HUGHES, J.V., ZOLTICK, P.W., and WILSON, J. (2000). Humoral immunity to adeno-associated virus type 2 vectors following administration to murine and nonhuman primate muscle. J. Virol. **74,** 2420–2425.

CLARK, K.R., and JOHNSON, P.R. (1998). rAAV vectors as an AIDS

vaccine. In *First Annual Meeting of American Society of Gene Therapy*, Seattle, Washington, May 28–31, 1998.

DANIEL, M.D., KIRCHHOFF, F., CZAJAK, S.C., SEHGAL, P.K., and DESROSIERS, R.C. (1992). Protective effects of a live attenuated SIV vaccine with a deletion in the *nef* gene. Science **258,** 1938–1941.

DURING, M.J., XU, R., YOUNG, D., KAPLIT, M., SHERWIN, R.S., and LEONE, P. (1998). Peroral gene therapy of lactose intolerance using an adeno-associated virus vector. Nat. Med. **4,** 1131–1135.

DURING, M.J., SYMES, C.M., LAWLOR, P.A., LIN, J., DUNNING, J., FITZSIMONS, H.L., POULSEN, D., LEONE, P., XU, R., DICKER, B.L., LIPSKI, J., and YOUNG, D. (2000). An oral vaccine against NMDR1 with efficacy in experimental stroke and epilepsy. Science **287,** 1453–1460.

ERIKSSON, K., KILANDER, A., HAGBERG, L., NORKRANS, G., HOLMGREN, J., and CZERKINSKY, C. (1993). Intestinal antibody responses to oral vaccination in HIV-infected individuals. AIDS **7,** 1087–1091.

FAN, D.S., OGAWA, M., FUJIMOTO, K.I., IKEGUCHI, K., OGASAWARA, Y., URABE, M., NISHIZAWA, M., NAKANO, I., YOSHIDA, M., NAGATSU, I., ICHINOSE, H., NAGATSU, T., KURITZMAN, G.J., and OZAWA, K. (1998). Behavioral recovery in 6-hydroxydopamine-lesioned rats by cotransduction of striatum with tyrosine hydroxylase and aromatic L-amino acid decarboxylase genes using two separate adeno-associated virus vectors. Hum. Gene Ther. **9,** 2527–2535.

FISHER, K.J., JOOSS, K., ALSTON, J., YANG, Y., HAECKER, S.E., HIGH, K., PATHAK, R., RAPER, S.E., and WILSON, J.M. (1997). Recombinant adeno-associated virus for muscle directed gene therapy. Nat. Med. **3,** 306–321.

FLOTTE, T.R., AFIONE, S.A., CONRAD, C., MCGRATH, S.A., SOLOW, R., OKA, H., ZEITLIN, P.L., GUGGINO, W.B., and CARTER, B.J. (1993). Stable in vivo expression of the cystic fibrosis transmembrane conductance regulator with an adeno-associated virus vector. Proc. Natl. Acad. Sci. U.S.A. **90,** 10613–10617.

HALBERT, C.L., RUTLEDGE, E.A., ALLEN, J.M., RUSSELL, D.W., and MILLER, A.D. (2000). Repeat transduction in the mouse lung by using adeno-associated virus vectors with different serotypes. J. Virol. **74,** 1524–1532.

HERR, W., LINN, B., LEISTER, N., WANDEL, E., BUSCHENFELDE, K.H.M.Z., and WOLFEL, T. (1997). The use of computer-assisted video image analysis for the quantification of $CD8^+$ T lymphocytes producing tumor necrosis factor a spots in response to peptide antigens. J. Immunol. Methods **203,** 141–152.

HERZOG, R.W., HAGSTROM, J.N., KUNG, S.H., TAI, S.J., WILSON, J.M., FISHER, K.J., and HIGH, K.A. (1997). Stable gene transfer and expression of human blood coagulation factor IX after intramuscular injection of recombinant adeno-associated virus. Proc. Natl. Acad. Sci. U.S.A. **94,** 5804–5809.

HOLLON, T. (2000). Researchers and regulators reflect on first gene therapy death. Nat. Med. **6,** 6.

KAY, M.A., MANNO, C.S., RAGNI, M.V., LARSON, P.L., COUTO, L.B., McCLELLAND, A., GLADER, B., CHEW, A.J., TAI, S.J., HERZOG, R.W., ARRUDE, V., JOHNSON, F., SCALLAN, C., SKARAGARD, E., FLAKE, A.W., and HIGH, K.A. (2000). Evidence for gene transfer and expression of factor IX in haemophilia B patients treated with an AAV vector. Nat. Genet. **24,** 257–261.

KEARNS, W.G., AFIONE, S.A., FULMER, S.B., PANG, M.C., ERIKSON, D., EGAN, M., LANDRUM, M.J., FLOTTE, T.R., and CUTTING, G.R. (1996). Recombinant adeno-associated virus (AAV-CFTR) vectors do not integrate in a site-specific fashion in an immortalized epithelial cell line. Gene Ther. **3,** 748–755.

KOTIN, R.M., SINISCALCO, M., SAMULSKI, R.J., ZHU, X.D., HUNTER, L., LAUGHLIN, C.A., MCLAUGHLIN, S., MUZYCZKA, N., ROCCHI, M., and BERNS, K.I. (1990). Site-specific integration by adeno-associated virus. Proc. Natl. Acad. Sci. U.S.A. **87,** 2211–2215.

LEWIN, A.S., DRENSER, K.A., HAUSWIRTH, W.W., NISHIKAWA, S., YASUMURA, D., FLANNERY, J.G., and LAVAIL, M.M. (1998). Ribozyme rescue of photoreceptor cells in a transgenic rat model of autosomal dominant retinitis pigmentosa. Nat. Med. **4,** 967–971.

LEWIS, D.E., TANG, D.S.N., ADU-OPPONG, A., SCHOBER, W., and RODGERS, J.R. (1994). Anergy and apoptosis in $CD8^+$ T cells from HIV-infected persons. J. Immunol. **153,** 412–420.

MANDL, C.W., ABERLE, J.H., ABERLE, S.W., HOLZMANN, H., ALLISON, S.L., and HEINZ, F.X. (1998). In vitro-synthesized infectious RNA as an attenuated live vaccine in a flavivirus model. Nat. Med. **4,** 1438–1440.

MANNING, W.C., PALIARD, X., ZHOU, S., PAT BLAND, M., LEE, A.Y., HONG, K., WALKER, C.M., ESCOBEDO, J.A., and DWARKI, V. (1997). Genetic immunization with adeno-associated virus vectors expressing herpes simplex virus type 2 glycoproteins B and D. J. Virol. **71,** 7960–7962.

MATANO, T., KANO, M., ODAWARA, T., NAKAMURA, H., TAKEDA, A., MORI, K., SATO, T., and NAGAI, Y. (2000). Induction of protective immunity against pathogenic simian immunodeficiency virus by a foreign receptor-dependent replication of an engineered avirulent virus. Vaccine **18,** 3310–3318.

MURPHEY-CORB, M. (1997). Live-attenuated HIV vaccines: How safe enough? Nat. Med. **3,** 17–18.

OZAWA, K. (1997). *Virology.* Hatanaka, S., ed. (Asakura Press, Tokyo, Japan) pp. 222–229.

PONNAZHAGAN, S., MUKHERJEE, P., WANG, X.-S., QING, K., DUBE, D.M., MAH, C., KURPAD, C., YODER, M.C., SPROUR, E.F., and SRIVASTAVA, A. (1997). Adeno-associated virus type 2-mediated transduction in primary human bone marrow-derived $CD34^+$ hematopoietic progenitor cells: Donor variation and correlation of transgene expression with cellular differentiation. J. Virol. **71,** 8262–8267.

PONNAZHAGAN, S., MAHENDRA, G., CURIEL, D.T., and SHAW, D.R. (2001). Adeno-associated virus type 2-mediated transduction of human monocyte-derived dendritic cells: implications for ex vivo immunotherapy. J. Virol. **75,** 9493–9501.

ROBINSON, H., MONTEFIORI, D.C., JOHNSON, R.P., MANSON, K.H., KALISHI, M.L., LIFSON, J.D., RIZVI, T.A., LU, S., HU, S.L., MAZZARA, G.P., PANICALI, D.L., HERNDON, J.G., GLICKMAN, R., CANDIDO, M.A., LYDY, S.L., WYAND, M.S., and MCCLURE, H.M. (1999). Neutralizing antibody-independent containment of immunodeficiency virus challenges by DNA priming and recombinant pox virus booster immunizations. Nat. Med. **5,** 526–534.

SARUKHAN, A., CAMUGLI, S., GJATA, B., BOEHMER, H.V., DANOS, O., and JOOSS, K. (2001). Successful interference with cellular immune responses to immunogenic proteins encoded by recombinant viral vectors. J. Virol. **75,** 267–277.

SCHNELL, M.J., FOLEY, H.D., SILER, C.A., MCGETTIGAN, J.P., DIETZACHOLD, B., and POMERANTZ, R.J. (2000). Recombinant rabies virus as potential live-viral vaccines for HIV-1. Proc. Natl. Acad. Sci. U.S.A. **97,** 3544–3549.

SFERRA, T.J., QU, G., MCNEELY, D., RENNARD, R., CLARK, K.R., LO, W.D., and JOHNSON, P.R. (2000). Recombinant adeno-associated virus-mediated correction of lysosomal storage within the central nervous system of the adult mucopolysaccharidosis type VII mouse. Hum. Gene Ther. **11,** 507–519.

SNYDER, R.O., MIAO, C.H., PATIJN, G.A., SPRATT, S.K., DANOS, O., NAGY, D., GOWN, A.M., WINTHER, B., MEUSE, L., COHEN, L.K., THOMPSON, A.R., and KAY, M.A. (1997). Persistent and therapeutic concentrations of human factor IX in mice after hepatic gene transfer of recombinant AAV vectors. Nat. Genet. **16,** 270–276.

VILLACRES, M.C., ZUO, J., and BERGMANN, C.C. (2000). Maintenance of $CD8^+$ T-cell memory following infection with recombinant sindbis and vaccinia viruses. Virology **270,** 54–64.

XIAO, X., LI, J., and SAMULSKI, R.J. (1996). Efficient long-term gene transfer into muscle tissue of immunocompetent mice by adeno-associated virus vector. J. Virol. **70,** 8098–8108.

XIN, K.Q., URABE, M., YANG, J., NOMIYAMA, K., MIZUKAMI, H., HAMAJIMA, K., NOMIYAMA, H., SAITO, T., IMAI, M., MONAHAN, J., OKUDA, K., OZAWA, K., and OKUDA, J. (2001). A novel recombinant adeno-associated virus vaccine induces a long-term humoral immune response to HIV. Hum. Gene Ther. **12,** 1047–1061.

XIN, K.-Q., SASAKI, S., KOJIMA, Y., JOUNAI, N., KUMAMOTO, Y., HASHIMOTO, K., SHINODA, K., HAMAJIMA, K., and OKUDA, K. (2002). Detection of progeny immune responses after intravenous administration of DNA vaccine to pregnant mice. Biol. Procedures Online **3,** 91–101 (www.biologicalprocedures.com).

YOSHIDA, T., OKUDA, K., XIN, K.Q., FUKUSHIMA, J., TODA, S., HAGIWARA, E., HAMAJIMA, K., KOSHINO, T., and SAITO, T. (2001). Activation of HIV-1-specific immune responses to an HIV-1 vaccine constructed from a replication-defective adenovirus vector using various combinations of immunization protocols. Clin. Exp. Immunol. **124,** 445–452.

ZHANG, Y., CHIRMULE, N., GAO, G.-P., and WILSON, J. (2000). CD40 ligand-dependent activation of cytotoxic T lymphocytes by adeno-associated virus vectors in vivo: role of immature dendritic cells. J. Virol. **74,** 8003–8010.

Address reprint requests to:
Dr. Kenji Okuda
Department of Bacteriology
Yokohama City University School of Medicine
3-9 Fukuura, Kanazawa-ku, Yokohama 236, Japan

E-mail: kokuda@med.yokohama-cu.ac.jp

Received for publication January 8, 2002; accepted after revision July 16, 2002.

Published online: August 7, 2002.

The Journal of Neuroscience, August 15, 2002, 22(16):6920–6928

Neuroprotective Effects of Glial Cell Line-Derived Neurotrophic Factor Mediated by an Adeno-Associated Virus Vector in a Transgenic Animal Model of Amyotrophic Lateral Sclerosis

Li-Jun Wang,[1,2] Yan-Yan Lu,[1,2] Shin-ichi Muramatsu,[1] Kunihiko Ikeguchi,[1] Ken-ichi Fujimoto,[1] Takashi Okada,[2] Hiroaki Mizukami,[2] Takashi Matsushita,[2] Yutaka Hanazono,[2] Akihiro Kume,[2] Toshiharu Nagatsu,[3] Keiya Ozawa,[2] and Imaharu Nakano[1]

[1]Division of Neurology, Department of Medicine and [2]Division of Genetic Therapeutics, Center for Molecular Medicine, Jichi Medical School, Minamikawachi-machi, Tochigi 329-0498, Japan, and [3]Institute for Comprehensive Medical Science, Fujita Health University, Toyoake, Aichi 470-1192, Japan

The Journal of Neuroscience, August 15, 2002, 22(16):6920–6928

Neuroprotective Effects of Glial Cell Line-Derived Neurotrophic Factor Mediated by an Adeno-Associated Virus Vector in a Transgenic Animal Model of Amyotrophic Lateral Sclerosis

Li-Jun Wang,[1,2] Yan-Yan Lu,[1,2] Shin-ichi Muramatsu,[1] Kunihiko Ikeguchi,[1] Ken-ichi Fujimoto,[1] Takashi Okada,[2] Hiroaki Mizukami,[2] Takashi Matsushita,[2] Yutaka Hanazono,[2] Akihiro Kume,[2] Toshiharu Nagatsu,[3] Keiya Ozawa,[2] and Imaharu Nakano[1]

[1]Division of Neurology, Department of Medicine and [2]Division of Genetic Therapeutics, Center for Molecular Medicine, Jichi Medical School, Minamikawachi-machi, Tochigi 329-0498, Japan, and [3]Institute for Comprehensive Medical Science, Fujita Health University, Toyoake, Aichi 470-1192, Japan

Amyotrophic lateral sclerosis (ALS) is a relentlessly progressive lethal disease that involves selective annihilation of motoneurons. Glial cell line-derived neurotrophic factor (GDNF) is proposed to be a promising therapeutic agent for ALS and other motor neuron diseases. Because adeno-associated virus (AAV) has been developed as an attractive gene delivery system with proven safety, we explored the therapeutic efficacy of intramuscular delivery of the GDNF gene mediated by an AAV vector (AAV-GDNF) in the G93A mouse model of ALS. We show here that AAV-GDNF leads to substantial and long-lasting expression of transgenic GDNF in a large number of myofibers with its accumulation at the sites of neuromuscular junctions. Detection of GDNF labeled with FLAG in the anterior horn neurons, but not β-galactosidase expressed as a control, indicates that most of the transgenic GDNF observed there is retrogradely transported GDNF protein from the transduced muscles. This transgenic GDNF prevents motoneurons from their degeneration, preserves their axons innervating the muscle, and inhibits the treated-muscle atrophy. Furthermore, four-limb injection of AAV-GDNF postpones the disease onset, delays the progression of the motor dysfunction, and prolongs the life span in the treated ALS mice. Our finding thus indicates that AAV-mediated GDNF delivery to the muscle is a promising means of gene therapy for ALS.

Key words: amyotrophic lateral sclerosis; motoneuron; adeno-associated virus vector; glial cell line-derived neurotrophic factor; gene therapy; retrograde transport

Amyotrophic lateral sclerosis (ALS) is one of the most tragic neurodegenerative diseases affecting motoneurons. Because the mechanism leading to motoneuron degeneration in ALS is not understood, currently there is no therapy available to prevent or cure ALS. Approximately 20% of familial ALS is linked to mutations in the Cu/Zn superoxide dismutase (SOD1) gene (Julien, 2001), transgenic mice overexpressing this mutant (mSOD1G93A) gene found to develop a dominantly inherited adult-onset paralytic disorder that has many of the clinical and pathological features of familial ALS (Gurney et al., 1994).

Glial cell line-derived neurotrophic factor (GDNF), which has been demonstrated to be the most potent neurotrophic factor for the proliferation, differentiation, and survival of spinal motoneurons, exhibits very good therapeutic potential for ALS (Henderson et al., 1994; Oppenheim et al., 1995; Yan et al., 1995; Sagot et al., 1996; Bohn, 1999; Mohajeri et al., 1999). Systemic administration of GDNF as a recombinant protein to ALS patients, however, is not beneficial, because of its short plasma half-life and poor access to motoneurons, on the one hand, and, on the other hand, because of its severe side effects that prevent its administration at an adequate dose (Haase et al., 1997; Alisky and Davidson, 2000). If ways that make continuous and motoneuron-confined delivery of GDNF possible are established, the disadvantages of its systemic administration will be overcome. Gene therapy involving the injection of a vector encoding a gene for GDNF into skeletal muscles will be a good candidate for such a method.

Three different viral vectors have been examined to transfer different genes to different tissues for ALS gene therapy (Alisky and Davidson, 2000). An adeno-associated virus (AAV) vector is one of the most attractive gene delivery vehicles and one that might be more practical with respect to safety. Skeletal muscle is a good platform for gene delivery (Xiao et al., 1996), and only at neuromuscular junctions (NMJs) are the nerve terminals in contact with myofibers, in which a barrier against various substances is absent, allowing them to reach the CNS. Furthermore, intramuscular injection is much safer and easier compared with intraspinal injection. Indeed, muscle-directed gene therapy mediated by an AAV vector has led to tremendous success in

Received Feb. 20, 2002; revised May 13, 2002; accepted May 13, 2002.

This study was supported in part by the following: a Grant-in-Aid for Scientific Research on Priority Areas and Special Coordination Funds for Promoting Science and Technology from the Ministry of Education, Culture, Sports, Science and Technology, The Japanese Government; by Health Sciences Research Grants from the Ministry of Health Labour and Welfare of Japan; by Core Research for Evolutional Science and Technology of Japan Science and Technology Corporation; by Research on Neurodegenerative Diseases, Health Science Research Grants from the Ministry of Health, Labor and Welfare; and by a Grant-in-Aid for Research on Specific Diseases from the Ministry of Health, Labour and Welfare of Japan. We thank Yaeko Nagatsuka and Yoshie Sato for their excellent technical assistance. We thank Masashi Urabe and Dongsheng Fan for the helpful advice. We also thank Avigen Inc. for providing the AAV vector production system.

Correspondence should be addressed to either Dr. Imaharu Nakano or Dr. Shin-ichi Muramatsu, Division of Neurology, Department of Medicine, Jichi Medical School, 3311-1 Yakushiji, Minamikawachi-machi, Tochigi 329-0498, Japan. E-mails: inakano@ms.jichi.ac.jp and muramats@ms.jichi.ac.jp.

Y.-Y. Lu's present address: Stem Cell Research Center, Health Science Center, Peking University, Beijing 100083, China.

 0270-6474/02/226920-09$15.00/0

numerous animal models of human diseases (Li et al., 1999; Kay et al., 2000; Wang et al., 2000).

Given the existence of endogenous GDNF in muscles and the spinal cord and its upregulation in ALS patients (Yamamoto et al., 1996; Golden et al., 1998; Suzuki et al., 1998; Grundstrom et al., 1999), we constructed the AAV-GDNF vector expressing a GDNF-FLAG fusion protein that can be readily distinguished from the endogenous one with FLAG. We showed that the intramuscular administration of an AAV vector harboring the GDNF gene to ALS mouse models can significantly delay the onset of disease, lengthen the life span, abate the behavioral impairment, and promote motoneuron survival. Moreover, we obtained direct evidence that the product of GDNF boosted by gene delivery in the muscle is retrogradely transported to the motoneurons of the spinal cord.

MATERIALS AND METHODS

Administration of an AAV vector. Male transgenic mice with the G93A human SOD1 mutation (SOD1G93A) were obtained from The Jackson Laboratory (Bar Harbor, ME). AAV vector plasmid pAAV-GDNFflag contains mouse GDNF cDNA tagged with a FLAG sequence (DYKDDDDK) at the C terminus under the human cytomegalovirus immediate-early promoter, with the human growth hormone first intron and simian virus 40 polyadenylation signal sequence between the inverted terminal repeats of the AAV type 2 genome (Wang et al., 2002). AAV vector plasmid pAAV-LacZ, auxiliary plasmid pHLP19, and pladenol were described previously (Matsushita et al., 1998). AAV vectors were produced in human embryonic kidney 293 (HEK293) cells by triple transfection of vector plasmid and helper plasmids listed above as described previously (Wang et al., 2002). In brief, subconfluent HEK293 cells were transiently transfected by calcium phosphate method. Seventy-two hours after transfection, the cells were collected and subjected to three cycles of freeze–thaw lysis (alternating between dry-ice–ethanol and 37°C baths). AAV vectors were purified by two sequential continuous cesium chloride density gradients and estimated for final particle titer by quantitative DNA dot-blot hybridization. Before administration, AAV vectors were diluted in PBS to 1×10^{11} genome copies/100 μl. At 9 weeks of age, ALS mice were randomly assigned to one treatment group that was injected with AAV-GDNF vector ($n = 12$) or one of two control groups that were injected with AAV-LacZ vector ($n = 6$) and the vehicle ($n = 5$), respectively, into four limbs (gastrocnemius and triceps brachii muscles). The dosage was 30 μl for gastrocnemius and 20 μl for triceps brachii muscles. Because mice injected with AAV-LacZ vector and the vehicle were indistinguishable with regard to all variables tested during the experimental period, the two groups were considered as one control group for analysis. In another subgroup ($n = 7$), all of the mice had AAV-GDNF vector injected into the muscles of the left forelimbs and hindlimbs and AAV-LacZ vector into those of the right ones.

Behavioral testing and mortality. Mice were first given 3 d to become acquainted with the rotarod apparatus (Rota-Rod/7650; Ugo Basile, Comerio, Italy) before the test. For detection, mice were placed on the rotating rod at the speeds of 5, 10, and 20 rpm, and the time each mouse remained on the rod was registered automatically. The onset of disease was defined as the time when the mouse could not remain on the rotarod for 7 min at a speed of 20 rpm, as described previously (Li et al., 2000). If the mouse remained on the rod for >7 min, the test was completed and scored as 7 min. Mice were tested every 2 d until they could no longer perform the task. Mortality was scored as the age of death when the mouse was unable to right itself within 30 sec when placed on its back in a supine position (Li et al., 2000).

Tissue preparation. One week before being killed, mice were bilaterally injected with neural tracer cholera toxin subunit B (CTB) (0.1% in distilled H_2O, 3 μl; List Biologic, Campbell, CA) into gastrocnemius muscles to selectively label motoneurons that retained axons innervating the treated muscles. At the indicated times, gastrocnemius muscles were dissected out, weighed, rapidly frozen in liquid nitrogen-cooled isopentane, and then stored at − 80°C for immunohistochemistry or GDNF ELISA analysis. After dissecting out the muscles, the mice were perfused with ice-cold PBS, followed by 4% paraformaldehyde (PFA). The spinal cord was dissected out, postfixed for 4 hr in 4% PFA, and then cryoprotected sequentially in sucrose.

GDNF ELISA. To determine muscle GDNF levels, tissues were homogenized at a w/v ratio of 100 mg/ml in lysis buffer (137×10^{-3} mol/l NaCl, 20×10^{-3} mol/l Tris, pH 8.0, 1% NP-40, and 10% glycerol) containing protease and phosphatase inhibitors, ultrasonicated, and then centrifuged at 12,000 × *g*. The supernatants were acidified and neutralized to pH 7.4 before assaying. The tissue levels of GDNF were measured with an ELISA kit (GDNF Emax ImmunoAssay System; Promega, Madison, WI), according to the protocol of the supplier. The levels of GDNF were expressed as picograms per milligram of protein. The assay sensitivity ranged from 16 to 1000 pg/ml.

Immunohistochemistry. Muscle sections (10 μm) were fixed in cold acetone, followed by incubation with rabbit anti-FLAG polyclonal antibodies (1:1000; Sigma, St. Louis, MO) as primary antibodies and biotinylated anti-rabbit antibodies as secondary ones (1:400; Santa Cruz Biotechnology, Santa Cruz, CA). Sections were visualized by the avidin–biotin–peroxidase complex procedure (Vectastain ABC kits; Vector Laboratories, Burlingame, CA) using 3,3-diaminobenzidine as a chromogen.

For double-immunofluorescence staining of muscles, sections were sequentially incubated with blocking solution, polyclonal rabbit anti-FLAG antibodies (1:500; Sigma), FITC-conjugated goat anti-rabbit IgG (1:200; Santa Cruz Biotechnology), and tetramethylrhodamine-conjugated α-bungarotoxin (Molecular Probes, Eugene, OR). Sections were examined and photographed under a confocal laser scanning microscope (TCS NT; Leica, Heidelberg, Germany).

For morphological analysis of the spinal cord, serial transverse sections (30 μm) were obtained for Nissl, SMI-32, or CTB immunostaining. Free-floating sections were immunohistochemically stained for SMI-32 with a Mouse-on-Mouse kit (M.O.M kit) (Vector Laboratories, Burlingame, CA), according to the protocol of the manufacturer. Sections processed for CTB immunoreactivity were blocked with 5% rabbit serum, followed by incubation with anti-CTB antibodies (1:10000, goat antiserum to CTB; List Biologic). Sections were visualized by standard ABC methods.

For double immunostaining of the spinal cord, sections were blocked with 10% normal goat serum and the blocking solution supplied with the M.O.M kit for 1 hr, respectively, and then sequentially incubated with polyclonal rabbit anti-FLAG antibodies (1:250; Sigma) and monoclonal mouse anti-SMI-32 antibodies (1:500) overnight at 4°C. After incubation with FITC-conjugated goat anti-rabbit IgG (mouse absorbed, 1:200; Santa Cruz Biotechnology) and rhodamine-conjugated goat anti-mouse IgG (1:200; Santa Cruz Biotechnology) for 2 hr at room temperature, the sections were examined and photographed under confocal laser scanning microscope.

Morphometric analysis and cell counting. Morphometric analysis was performed on images captured with a CCD camera using KS 400 image analysis software (Zeiss, Oberkochen, Germany). The mean area of muscle fibers was calculated from counts of >1000 fibers in randomly selected areas. To compare the number of motoneurons in the spinal cord, we counted neurons in Nissl-stained and SMI-32- and CTB-immunostained sections spanning the cervical and lumbrosacral enlargements in each group, as described previously (Lewis et al., 2000). For each mouse, at least 20 sections in each sixth serial section were subjected to counting. Only large cell profiles meeting the following criteria were included: location in the ventral horn below a lateral line from the central canal, containing a distinct nucleus with a nucleolus, and possession of at least one thick process.

Statistical analyses. The data were statistically analyzed using repeated-measures ANOVA, followed by a Tukey's honestly significance difference test for multiple comparisons between groups (StatView 5.0 software; SAS, Cary, NC).

RESULTS

GDNF transgene expression in muscles of ALS mice

We determined the amount of GDNF in gastrocnemius muscles by ELISA. At 110 d of age (7 weeks after injection), the GDNF levels in AAV-GDNF vector-treated mice were 7985.0 ± 874.0 pg/mg protein, which is >120-fold higher than that in the control ALS group (62.2 ± 20.5 pg/mg protein; $p < 0.01$; $n = 4$). At the time of death, AAV-GDNF vector-treated ALS mice tended to show a decrease in intramuscular GDNF expression (3281.7 ± 667.0 pg/mg protein; $n = 4$). We assumed that the reduction of GDNF was attributable to the severe atrophy of the transduced

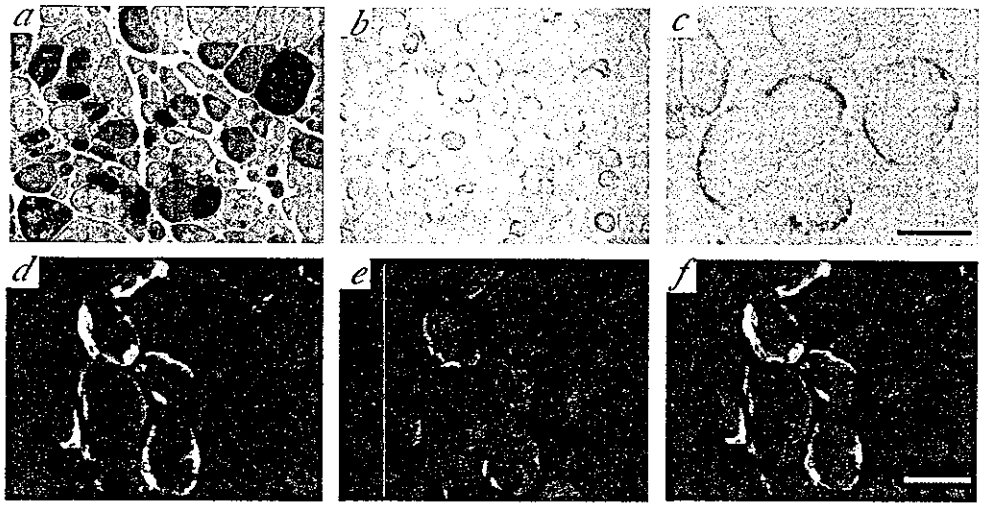

Figure 1. Characterization and muscle expression of AAV vector-transduced genes after injection into gastrocnemius muscles. 5-Bromo-4-chloro-3-indolyl-β-D-galactopyranoside-stained cross sections from control ALS mice after an injection with AAV-LacZ vector at 110 d of age (*a*). FLAG immunoreactivity is observed around the injection sites in AAV-GDNF vector-treated ALS mice of the same age (*b*; low magnification). At higher magnification (*c*), intense immunoreactivity can be seen to be mainly localized in the vicinity of the sarcolemma as well as surrounding regions, suggesting secreted expression of transgene-derived GDNF after intramuscular AAV-GDNF vector injection. More intense immunoreactivity for FLAG (*d*) was localized to postsynaptic AChR-rich regions, as confirmed by double staining with rhodamine-labeled α-bungarotoxin (*e*), indicating the accumulation of transgene-derived GDNF at neuromuscular junctions. *f*, Merging of *c* and *d*. Scale bars: (in *c*) *a*, 100 μm; *b*, 200 μm; *c*, 50 μm; (in *f*) *d–f*, 50 μm.

muscle fibers in ALS mice, because stable GDNF expression can last for at least 8 months in age-matched wild-type mice (our unpublished data). These data suggested that AAV-GDNF vector could drive substantial transgenic GDNF expression in ALS mice until the end stage of the disease.

We next investigated the pattern of distribution of transgenic GDNF in muscles by means of immunodetection. Here, FLAG was used as a tag to distinguish transgenic GDNF from its endogenous counterpart. In AAV-GDNF vector-injected mice, strong FLAG immunoreactivity was detected in a large number of myofibers, both at 110 d of age and at the end stage of the disease. Punctured and reticular staining was observed in transverse sections of muscles, with intense immunoreactivity mainly localized in the vicinity of the sarcolemma, indicating that transgene-derived GDNF was efficiently secreted into the surrounding regions (Fig. 1*b*,*c*). Substantial FLAG signals could still be detected in atrophied myofibers at the end stage of the disease.

Furthermore, we performed double-immunofluorescence staining with anti-FLAG antibodies and α-bungarotoxin. α-Bungarotoxin is a molecular probe that specifically binds to the acetylcholine receptor (AChR) with high affinity on the postsynaptic membranes of NMJs. The results showed that more intense immunoreactivity for FLAG was colocalized with α-bungarotoxin signals, indicating that transgenic GDNF was concentrated primarily in the regions of NMJs (Fig. 1*d–f*). As expected, the muscles treated with AAV-LacZ vector or the vehicle exhibited no immunostaining for anti-FLAG at any time point.

Preservation of vector-treated muscles

At 110 d of age, the gastrocnemius muscles in the control ALS mice weighed only approximately half those in the age-matched wild-type mice (95.8 ± 19.4 vs 183.0 ± 22.2 mg; $n = 5$). However, the gastrocnemius muscles of AAV-GDNF vector-treated ALS mice were ~1.68 times (160.1 ± 32.9 mg; $p < 0.01$; $n = 5$) heavier than those of control ALS mice at the same age.

Histological analysis of muscles in control ALS mice at 110 d of age revealed widespread groups of small, acutely angulated fibers, consistent with severe neurogenic atrophy (Fig. 2*b*). The mean myofiber area was greatly decreased (1053.8 ± 581.0 μm^2; $n = 4$), being ~30% of that in age-matched wild-type mice (3517.6 ± 613.5 μm^2; $n = 5$). In contrast, the muscles treated with AAV-GDNF vector showed little evidence of neurogenic atrophy with a more consistent fiber size (Fig. 2*c*), the mean myofiber area (2252.8 ± 1035.2 μm^2; $n = 5$) reaching ~71% of that in wild-type mice and more than two times that in the control ALS group. Additionally, the notable shift of myofibers toward a smaller diameter observed in control ALS mice was evidently moderated in the AAV-GDNF vector-treated group (Fig. 2*d*), and the percentage of atrophied myofibers of <20 μm was significantly decreased (24% in control ALS group vs 9% in AAV-GDNF-treated group).

Retrograde transport of transgenic GDNF into spinal motoneurons

Retrograde axonal transport of GDNF into spinal lumbar motoneurons has been demonstrated in adult rats (Leitner et al., 1999). Here we examined whether or not transgenic GDNF could also be retrogradely transported to spinal motoneurons in ALS mice. For this purpose, we took advantage of the FLAG tag in transgenic GDNF to avoid interference of the results by endogenous GDNF. SMI-32 is a well characterized antibody that specifically recognizes nonphosphorylated neurofilaments (NP-NFs) and therefore serves as a reliable marker for motoneurons (Carriedo et al., 1996). Thus, we performed double immunostaining with SMI-32 and FLAG antibodies on spinal cord sections from ALS mice. At 110 d of age, FLAG immunosignals could be detected in SMI-32-positive cells in the corresponding ventral horn in ALS mice at 7 weeks after intramuscular AAV-GDNF vector injection, whereas no FLAG signal was detected in the spinal cords of the control group ALS mice. This was further demonstrated in the subgroup of unilaterally treated ALS mice; FLAG signals could only be detected in motoneurons of the ventral horn ipsilateral to the AAV-GDNF vector-injected side (Fig. 3*a–c*) and none in those on the contralateral AAV-LacZ vector-injected side. Although β-galactosidase signals were widely detected in AAV-LacZ vector-injected muscles, they were not observed at all in the corresponding ventral horn of the spinal cord.

Effect of transgenic GDNF on spinal motoneuron survival

To assess the neuroprotective effect of GDNF on the survival of motoneurons, we compared the numbers of spinal motoneurons in the different groups at 110 d of age. Nissl staining of the spinal

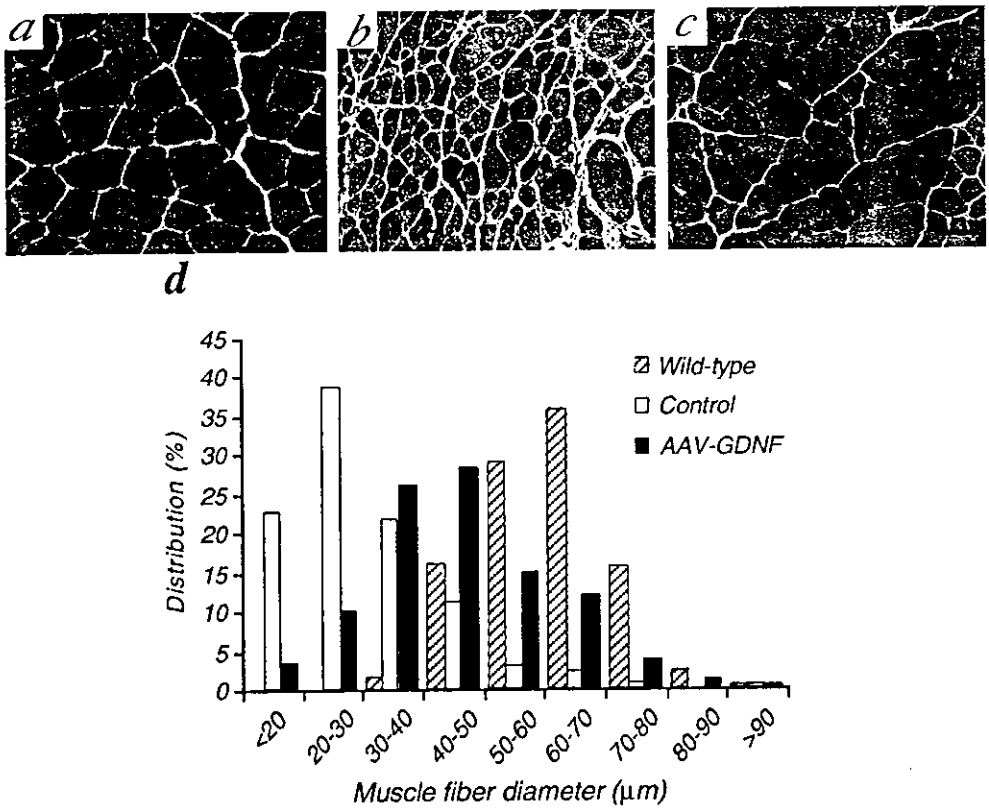

Figure 2. Photomicrographs of sections of gastrocnemius muscles from ALS mice at 110 d of age. *a*, Wild-type mouse. Note that large groups of angulated and atrophic muscle fibers were observed in control ALS mice (*b*), suggesting severe neurogenic atrophy in these mice. However, AAV-GDNF vector treatment markedly attenuated this denervation atrophy (*c*), consistent with a greater fiber area and a decreased shift in fiber size toward smaller ones (*d*) compared with in control ALS mice. Scale bar, 100 μm.

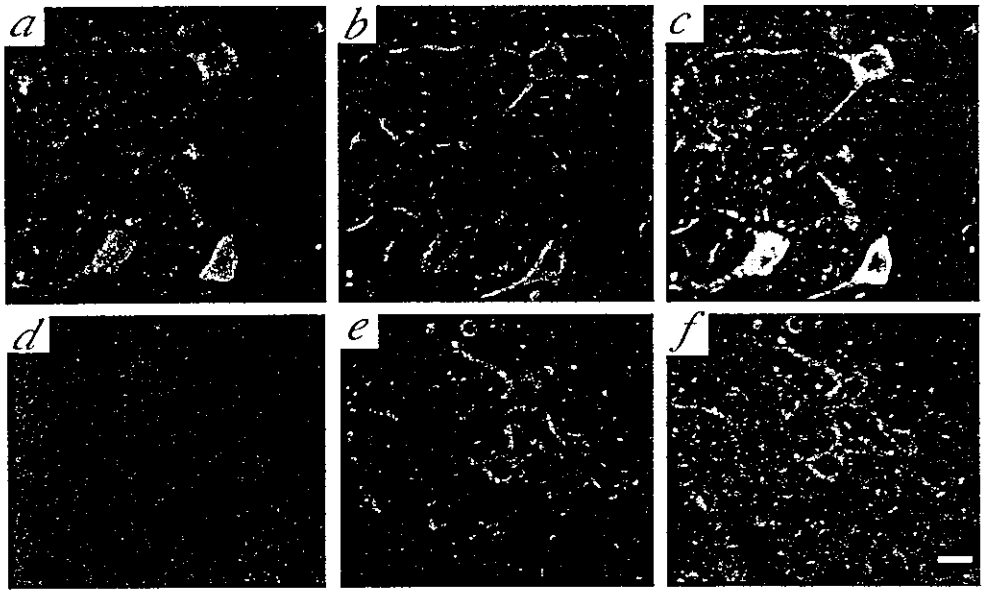

Figure 3. The retrograde transport of transgene-derived GDNF in motoneurons of the spinal cord. At 110 d of age (7 weeks after vector administration), transgene-derived GDNF was detected in the ventral horn of the corresponding spinal cord ipsilateral to the AAV-GDNF vector-injected side on double-immunofluorescence staining with anti-FLAG (*a*) and SMI-32 (*b*) antibodies. Merging of *a* and *b* showed colocalization of FLAG and SMI-positive neurons in the anterior horns, suggesting that the retrograde transport of transgene-derived GDNF occurred in motoneurons (*c*). *d–f*, The contralateral side injected with AAV-LacZ vector. Scale bar, 20 μm.

cord showed a severe loss of motoneurons in the ventral horns of the control ALS mice (Fig. 4*b*,*g*). In contrast, in AAV-GDNF vector-treated mice, a significantly larger number of motoneurons remained in both cervical and lumbar segments (Fig. 4*c*,*g*), suggesting a markedly protective effect of the transgenic GDNF on motoneurons.

Staining for NP-NF is a reliable means of assessing the extent of motoneuron loss in ALS, in which it has been shown that motoneuron degeneration induces dephosphorylation of NP-NF, resulting in SMI-32 staining resistance (Tsang et al., 2000). We performed this staining on serial sections to evaluate motoneurons with NP-NF. Consistent with the Nissl-staining results, AAV-GDNF vector-treated ALS mice had significantly greater numbers of SMI-32-positive motoneurons compared with in the control ALS group (Fig. 4*d–f*,*h*). Thus, the motoneuron degeneration, as well as the aberrant NF dephosphorylation in the spinal cord ventral horn of ALS mice, is also significantly inhibited after AAV-GDNF vector administration.

In the unilaterally treated subgroup of ALS mice killed at 110 d of age, many more motoneurons survived in the lumbar spinal cord ventral horns ipsilateral to the AAV-GDNF vector-injected side than on the contralateral side treated with AAV-LacZ vector

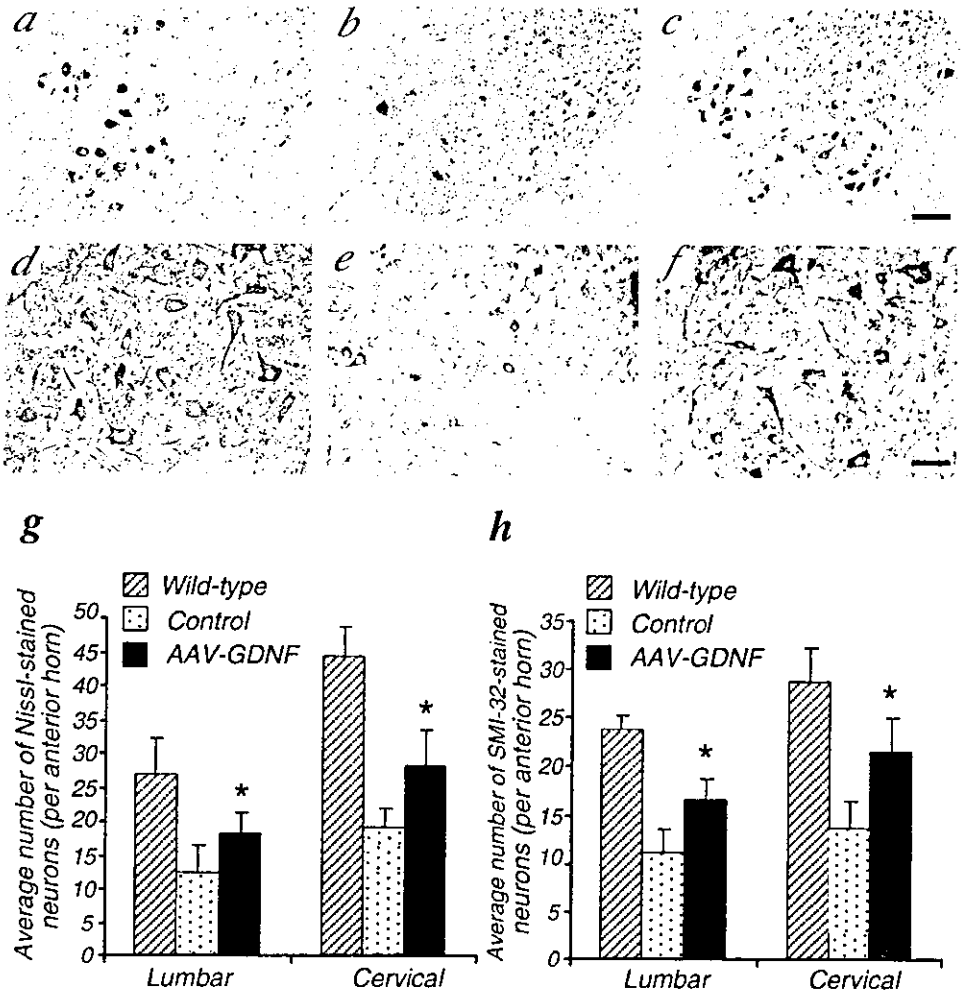

Figure 4. AAV-GDNF treatment significantly inhibits the loss of spinal motoneurons in ALS mice. Nissl staining (*a–c*) and SMI-32 immunochemistry (*d–f*) in wild-type (*a*, *d*), control (*b*, *e*), and AAV-GDNF vector-treated (*c*, *f*) ALS mice at 110 d of age after intramuscular injection. Scale bars: *a–c*, 100 μm; *d–f*, 50 μm. *g* and *h* show the significant presence of both Nissl-stained and SMI-32-positive motoneurons in the ventral horns of the spinal cord, respectively ($n = 4$; $^*p < 0.01$). The data represent the average numbers of neurons per anterior horn.

(Nissl staining, 17.1 ± 3.2 vs 10.3 ± 1.1; SMI-32-positive neurons, 15.6 ± 1.8 vs 8.8 ± 3.2; $p < 0.01$; $n = 5$). Thus, these findings further suggested that the therapeutic effect on motoneurons resulted from retrograde transport of transgenic GDNF on the same side rather than from systemic delivery.

Effect on the maintenance of motoneuron axonal projections to muscles

To further quantitatively assess surviving motoneurons that retained functioning neuromuscular projections to the injected muscles, we selectively labeled such motoneurons by injection of a neural tracer CTB into the bilateral gastrocnemius muscles of mice 1 week before being killed. At 110 d of age, there were much fewer CTB-labeled motoneurons in control ALS mice than those in wild-type mice. However, with AAV-GDNF vector treatment, more CTB-labeled motoneurons were maintained than in the control ALS group (20.7 ± 4.9 vs 11.0 ± 2.5%; $n = 4$; $p < 0.01$) (Fig. 5*d*). Transgenic GDNF delivery to muscle thus played an important role in the maintenance of the axonal projections of corresponding motoneurons.

For more accurate morphometric evaluation of surviving motoneurons labeled with CTB, we next determined the size and distribution of such neurons in the lumbar spinal cord. The control group of ALS mice killed at 110 d of age exhibited a significantly smaller mean area of CTB-labeled neurons than that in age-matched wild-type mice (353.1 ± 173.8 vs 733.7 ± 252.0 μm^2; $n = 4$; $p < 0.01$), the size distribution being shifted toward smaller ones, indicating significant atrophy of CTB-positive motoneurons (Fig. 5*e*). In contrast, AAV-GDNF vector treatment of ALS mice markedly decreased the motoneuron atrophy (605.8 ± 248.2 μm^2; $n = 4$; $p < 0.01$ vs control group), and the size distribution shifted toward smaller ones. Together, these results may directly show that GDNF gene delivery to muscles can promote the survival and inhibit the atrophy of motoneurons with axonal projections to target muscles in ALS mice.

GDNF delays the onset of disease, improves motor performance, and prolongs survival in transgenic ALS mice

Any group of ALS mice that had AAV-GDNF vector, AAV-LacZ vector, or the vehicle injected in the four limbs at 9 weeks of age showed similar motor performance, as quantified with a rotarod, until 12 weeks of age. Thereafter, it deteriorated quickly in control ALS mice, whereas the performance deterioration was significantly delayed in AAV-GDNF vector-treated mice ($p < 0.05$) (Fig. 6*a–c*), indicating significantly prolonged maintenance of their motor strength.

The average age of motor deficit onset in AAV-GDNF vector-treated ALS mice was 114.0 ± 4.0 d ($n = 12$), whereas it was 101.3 ± 5.4 d ($n = 11$) in control ALS mice, the difference being significant ($p < 0.01$) (Fig. 6*a*). AAV-GDNF vector treatment prolonged the mean survival by 16.6 ± 4.1 d compared with in the control ALS mice (138.9 ± 9.2 d in AAV-GDNF vector-treated mice vs 122.3 ± 5.7 d in control ALS mice; $n = 8$; $p < 0.01$) (Fig.

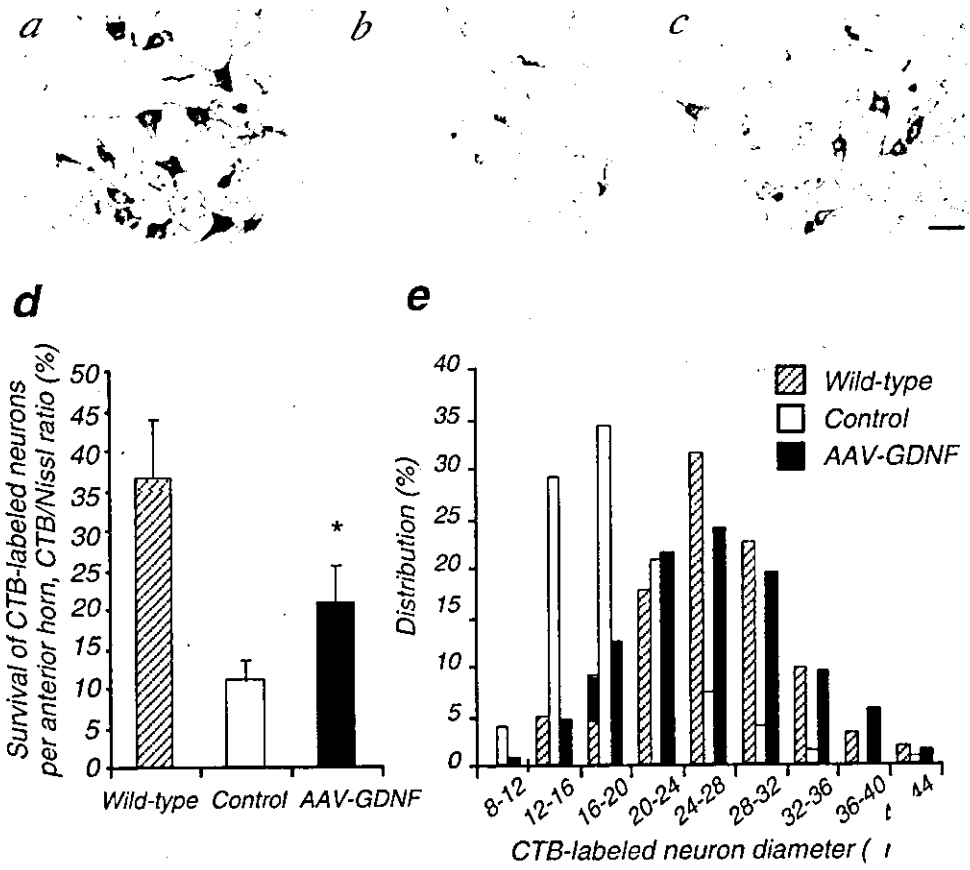

Figure 5. Effect of GDNF on motoneurons that retained axonal projections. CTB-labeled motoneurons in the ventral horns at 110 d of age in wild-type (*a*), control (*b*), and AAV-GDNF vector-treated (*c*) ALS mice after intramuscular injection. Scale bar, 50 μm. Note that AAV-GDNF vector-treated mice had significantly more large CTB-labeled motoneurons than control ALS mice (*d*). The value represents the CTB/Nissl ratio (average number of neurons per anterior horn). The shift in motoneuron size toward a smaller diameter was markedly retarded in AAV-GDNF vector-treated mice compared with in control ALS mice (*e*).

6*e*). These results mean that bilateral intramuscular injection of AAV-GDNF vector delayed the onset of disease by ~13% and prolonged the survival of transgenic ALS mice by ~14%.

However, weakness and atrophy of the skeletal muscles, especially in the hindlimbs, ultimately developed in all mice of all groups once motor symptoms had appeared. The duration of the disease, as evaluated as the number of days that elapsed from the onset to the end stage, did not differ between the AAV-GDNF vector-treated and control ALS mice (24.0 ± 3.5 vs 21.0 ± 3.5 d; $p > 0.05$).

Because GDNF is a secreted protein, we assessed whether the therapeutic benefit of transgene-derived GDNF also resulted from systemic circulation after AAV-GDNF vector administration or not. In a subgroup of unilaterally treated ALS mice that had AAV-GDNF vector injected into their left limbs and AAV-LacZ vector injected into their right ones, each mouse moved the AAV-GDNF vector-injected limbs almost normally until 110 d of age. However, the contralateral limbs developed muscle weakness at as early as 93 d of age, there being a waddling gait. Despite the better motor functions of AAV-GDNF vector-treated limbs, the mice showed no significant difference in the running time on a rotarod at any speed tested compared with the control ALS mice (data not shown). The average onset time of motor deficit in this subgroup also showed no significant difference compared with in the control ALS group (102.7 ± 3.1 d; $n = 7$; $p > 0.05$) (Fig. 6*d*).

DISCUSSION

We report here that intramuscular injection of AAV-GDNF vector into the transgenic ALS mice model results in sustained substantial biosynthesis of GDNF in the muscles, with findings demonstrating its retrograde transport to the corresponding spinal motoneurons. Furthermore, this transgene expression not only significantly prevents the loss of motoneurons but also leads to marked attenuation of the manifestation of the disease and prolongs survival of the transgenic ALS mice.

Here, we demonstrated substantial expression of the GDNF transgene after an intramuscular AAV-GDNF vector injection, which is sustained until the terminal stage in ALS mice, thus probably guaranteeing a continual supply of biologically synthesized GDNF to the motoneuronal axon terminals in the muscles. This will well meet the demands for long-term availability of therapeutic factors that is necessary because of the chronicity and progression of ALS. Although we failed to detect transgenic GDNF in the spinal cord at the death stage in ALS mice, this is probably attributable to severe loss of motoneurons or/and the impaired capacity of axonal transport at the end stage (Warita et al., 1999; Williamson and Cleveland, 1999).

It has been assumed that the neuroprotective effect of GDNF on motoneurons is based on its retrograde axonal transport from a target tissue to neuronal cell bodies, but no direct evidence for this hypothesis in gene therapy has been presented yet (Mohajeri et al., 1999; Alisky and Davidson, 2000). We successfully detected transgenic GDNF in spinal neurons of the ventral horn ipsilateral to the AAV-GDNF-injected side. These cells are confirmed to be motoneurons by means of double immunofluorescence. Because the antibody we used recognizes the FLAG epitope tagging transgenic GDNF, the interference with this result by endogenous GDNF in the spinal cord is excluded.

The transgenic GDNF that appeared in the motoneurons may have been derived through three possible ways: systemic delivery, retrograde transport of AAV vectors, or retrograde transport of

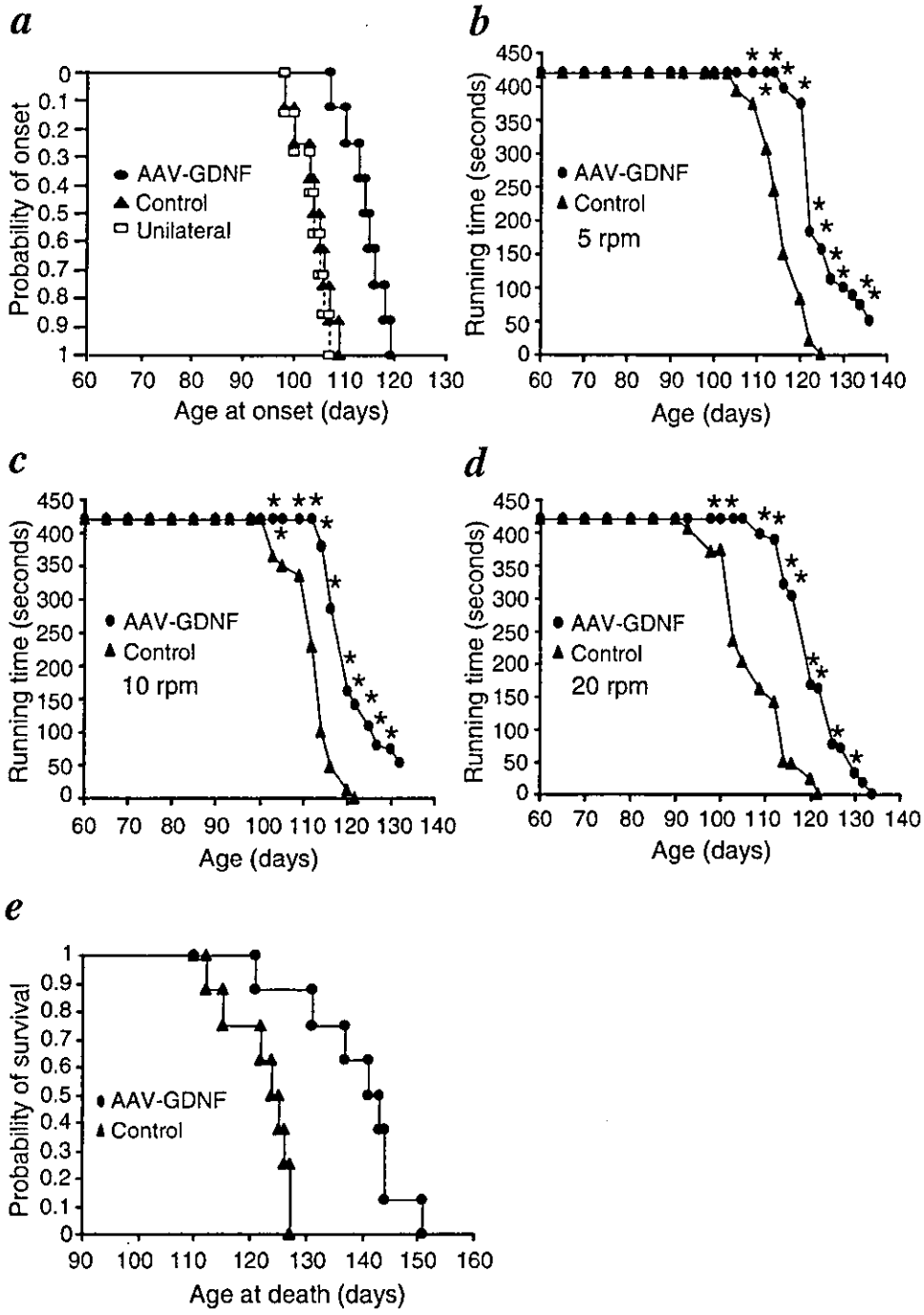

Figure 6. *a*, General behavior test for ALS mice. Cumulative probability of onset of rotarod deficits in ALS mice. The AAV-GDNF vector-treated mice had an age of onset of 114.0 ± 4.0 d (n = 12) compared with 101.3 ± 5.4 d (n = 11) for control ALS mice and 102.7 ± 3.1 d (n = 7) for unilaterally AAV-GDNF vector-treated mice. AAV-GDNF vector treatment significantly delayed disease onset by ~13 d compared with in control ALS mice ($p < 0.01$), whereas the onset in unilateral AAV-GDNF vector-treated mice did not show a significant difference from that in control ALS mice. Performance of ALS mice in the rotarod test at 5 rpm (*b*), 10 rpm (*c*), and 20 rpm (*d*). AAV-GDNF vector-treated ALS mice performed significantly better than control ALS mice (n = 8; $^*p < 0.05$). *e*, Cumulative probability of survival. Survival was significantly prolonged by ~17 d in AAV-GDNF vector-treated ALS mice when compared with in control transgenic ALS littermates treated with the vehicle or AAV-LacZ vector (n = 8; $p < 0.01$).

GDNF fusion protein itself. The restricted distribution and ipsilateral presentation of transgenic GDNF in motoneurons, as well as its known inability to pass through the blood–brain barrier, exclude the possibility of its systematic delivery to the spinal cord. To date, most reports show that AAV vectors are not retrogradely transported or are transported in only a very limited manner (Chamberlin et al., 1998; Klein et al., 1998; Alisky et al., 2000). One recent report, however, has revealed retrograde transport of an AAV vector itself in the CNS, a reporter green fluorescent protein being used as a tracer (Kaspar et al., 2002). Thus, in our study we cannot completely role out the possibility that AAV particles may also have been transported to the corresponding motoneurons. The vectors carried to the motoneurons, however, are assumed to be very limited because no β-galactosidase was detected in the corresponding spinal motoneurons, despite its wide distribution in the transduced muscles.

In contrast, the transgenic GDNF is abundantly detected in both transduced muscles and the corresponding motoneurons after AAV-GDNF injection. This finding, combined with the previous reports as well as our observation for β-galactosidase activity, indicates that the transgenic GDNF in the motoneurons is mainly derived through retrograde axonal transport of the GDNF protein. This is consistent with a previous study (Kordower et al., 2000) and our recently published data for the nigrostriatal system (Wang et al., 2002), showing that transgenic GDNF is retrogradely transported. The finding that transgenic

GDNF in muscle fibers was predominantly accumulated to the regions of NMJs is also compatible with its retrograde transport hypothesized because it is in the axon terminals in which substances secreted from muscle fibers are taken up to be retrogradely transported.

Both SMI-32 staining and Nissl staining have confirmed significant rescue of motoneurons by AAV-GDNF vector delivery. Because CTB can be axonally transported to neuronal cell bodies in a retrograde direction and be detected throughout the neuronal cytoplasm (Llewellyn-Smith et al., 2000), the detection of CTB-positive motoneurons means that they maintain intact axonal connection with the AAV-GDNF vector-injected muscles. Thus, CTB labeling makes it possible to assess the effect of the transgenic GDNF on the spinal motoneurons more accurately than with Nissl or NP-NF staining alone. This method reveals greater numbers of larger spinal motoneurons labeled with CTB in AAV-GDNF vector-treated ALS mice. These findings together indicate that intramuscular injection of AAV-GDNF vector can delay the degeneration of motoneurons, thereby allowing prolonged functioning axons in ALS mice.

AAV-GDNF vector-treated ALS mice with four-limb injections, in contrast to the control ALS group, show much better behavioral performance, with delayed onset of disease and a prolonged life span, which is in agreement with the attenuation of the motoneuron pathology. In the subgroup with unilateral AAV-GDNF treatment, the therapeutic effects of GDNF on behavioral and pathological features are limited to the same treated side, with obvious deterioration of motor performance on the AAV-LacZ vector-treated side. However, the motor performance on a rotarod and the onset of disease remain similar to those in the control group. Thus, it is assumed that the therapeutic benefit mostly resulted from direct action of transgenic GDNF on motoneurons after its retrograde transport rather than from the systemic delivery.

Although bilateral administration of AAV-GDNF vector markedly delays the onset of disease and improves the survival of ALS mice, it fails to prolong the length of time from disease onset to death. What is more, despite the substantial expression of GDNF, the AAV-GDNF vector-treated mice ultimately reach the end stage, when morphological assessment demonstrates such severe atrophy of myofibers and massive loss of spinal motoneurons as in the control ALS mice (data not shown). It has been reported that pathological changes occur at asymptomatic stages in ALS mice, and massive motoneuron death occurs at the end stage (Dal Canto and Gurney, 1995; Wong et al., 1995; Mourelatos et al., 1996; Tu et al., 1996; Bruijn et al., 1998; Shibata et al., 1998). Thus, it is assumed that the transgenic GDNF only exhibits its protective function for motoneurons in ALS mice at asymptomatic stages when the ventral horns may have a mild pathology. Once the disease develops, however, GDNF gene therapy cannot effectively inhibit the massive motoneuron death or interfere with the rapidly inevitable progression of the disease. In this study, we began the treatment at the age of 9 weeks. Administration of GDNF at earlier times and/or together with other neurotrophic factors (Bilak et al., 2001) may lead to better results.

In summary, we showed that intramuscular injection of AAV-GDNF vector in ALS mice results in long-term expression of GDNF in muscles, bringing about obvious benefits in behavioral, functional, and pathological features. The transgenic GDNF protein observed in the spinal motoneurons suggests its retrograde transport from the nerve terminals to motoneuronal cell bodies. Together, these data imply that AAV-mediated GDNF delivery to muscle will be a promising means of gene therapy for ALS.

REFERENCES

Alisky JM, Davidson BL (2000) Gene therapy for amyotrophic lateral sclerosis and other motor neuron diseases. Hum Gene Ther 11:2315–2329.

Alisky JM, Hughes SM, Sauter SL, Jolly D, Dubensky Jr TW, Staber PD, Chiorini JA, Davidson BL (2000) Transduction of murine cerebellar neurons with recombinant FIV and AAV5 vectors. NeuroReport 11:2669–2673.

Bilak MM, Corse AM, Kuncl RW (2001) Additivity and potentiation of IGF-I and GDNF in the complete rescue of postnatal motor neurons. Amyotroph Lateral Scler Other Motor Neuron Disord 2:83–91.

Bohn MC (1999) A commentary on glial cell line-derived neurotrophic factor (GDNF). From a glial secreted molecule to gene therapy. Biochem Pharmacol 57:135–142.

Bruijn LI, Houseweart MK, Kato S, Anderson KL, Anderson SD, Ohama E, Reaume AG, Scott RW, Cleveland DW (1998) Aggregation and motoneuron toxicity of an ALS-linked SOD1 mutant independent from wild type SOD1. Science 281:1851–1854.

Carriedo SG, Yin HZ, Weiss JH (1996) Motoneurons are selectively vulnerable to AMPA/kainate receptor-mediated injury *in vitro*. J Neurosci 16:4069–4079.

Chamberlin NL, Du B, de Lacalle S, Saper CB (1998) Recombinant adeno-associated virus vector: use for transgene expression and anterograde tract tracing in the CNS. Brain Res 793:169–175.

Dal Canto MC, Gurney ME (1995) Neuropathological changes in two lines of mice carrying a transgene for mutant human Cu, Zn SOD, and in mice overexpressing wild type human SOD: a model of familial amyotrophic lateral sclerosis (FALS). Brain Res 676:25–40.

Golden JP, Baloh RH, Kotzbauer PT, Lampe PA, Osborne PA, Milbrandt J, Johnson Jr EM (1998) Expression of neurturin, GDNF, and their receptors in the adult mouse CNS. J Comp Neurol 398:139–150.

Grundstrom E, Askmark H, Lindeberg J, Nygren I, Ebendal T, Aquilonius SM (1999) Increased expression of glial cell line-derived neurotrophic factor mRNA in muscle biopsies from patients with amyotrophic lateral sclerosis. J Neurol Sci 162:169–173.

Gurney ME, Pu H, Chiu AY, Dal Canto MC, Polchow CY, Alexander DD, Caliendo J, Hentati A, Kwon YW, Deng HX, Chen W, Zhai P, Sufit RL, Siddique T (1994) Motoneuron degeneration in mice that express a human Cu, Zn superoxide dismutase mutation. Science 264:1772–1775.

Haase G, Kennel P, Pettmann B, Vigne E, Akli S, Revah F, Schmalbruch H, Kahn A (1997) Gene therapy of murine motor neuron disease using adenoviral vectors for neurotrophic factors. Nat Med 3:429–436.

Henderson CE, Phillips HS, Pollock RA, Davies AM, Lemeulle C, Armanini M, Simmons L, Moffet B, Vandlen RA, Simpson LC (1994) GDNF: a potent survival factor for motoneurons present in peripheral nerve and muscle. Science 266:1062–1064.

Julien JP (2001) Amyotrophic lateral sclerosis: unfolding the toxicity of the misfolded. Cell 104:581–591.

Kaspar BK, Erickson D, Schaffer D, Hinh L, Gage FH, Peterson DA (2002) Targeted retrograde gene delivery for neuronal protection. Mol Ther 5:50–56.

Kay MA, Manno CS, Ragni MV, Larson PJ, Couto LB, McClelland A, Glader B, Chew AJ, Tai SJ, Herzog RW, Arruda V, Johnson F, Scallan C, Skarsgard E, Flake AW, High KA (2000) Evidence for gene transfer and expression of factor IX in haemophilia B patients treated with an AAV vector. Nat Genet 24:257–261.

Klein RL, Meyer EM, Peel AL, Zolotukhin S, Meyers C, Muzyczka N, King MA (1998) Neuron-specific transduction in the rat septohippocampal or nigrostriatal pathway by recombinant adeno-associated virus vectors. Exp Neurol 150:183–194.

Kordower JH, Emborg ME, Bloch J, Ma SY, Chu Y, Leventhal L, McBride J, Chen EY, Palfi S, Roitberg BZ, Brown WD, Holden JE, Pyzalski R, Taylor MD, Carvey P, Ling Z, Trono D, Hantraye P, Deglon N, Aebischer P (2000) Neurodegeneration prevented by lentiviral vector delivery of GDNF in primate models of Parkinson's disease. Science 290:767–773.

Leitner ML, Molliver DC, Osborne PA, Vejsada R, Golden JP, Lampe PA, Kato AC, Milbrandt J, Johnson Jr EM (1999) Analysis of the retrograde transport of glial cell line-derived neurotrophic factor (GDNF), neurturin, and persephin suggests that in vivo signaling for the GDNF family is GFRalpha coreceptor-specific. J Neurosci 19:9322–9331.

Lewis J, McGowan E, Rockwood J, Melrose H, Nacharaju P, Van Slegtenhorst M, Gwinn-Hardy K, Paul Murphy M, Baker M, Yu X, Duff K, Hardy J, Corral A, Lin WL, Yen SH, Dickson DW, Davies P, Hutton M (2000) Neurofibrillary tangles, amyotrophy and progressive motor disturbance in mice expressing mutant (P301L) tau protein. Nat Genet 25:402–405.

Li J, Dressman D, Tsao YP, Sakamoto A, Hoffman EP, Xiao X (1999)

rAAV vector-mediated sarcogylcan gene transfer in a hamster model for limb girdle muscular dystrophy. Gene Ther 6:74–82.
Li M, Ona VO, Guegan C, Chen M, Jackson-Lewis V, Andrews LJ, Olszewski AJ, Stieg PE, Lee JP, Przedborski S, Friedlander RM (2000) Functional role of caspase-1 and caspase-3 in an ALS transgenic mouse model. Science 288:335–339.
Llewellyn-Smith IJ, Martin CL, Arnolda LF, Minson JB (2000) Tracer-toxins: cholera toxin B-saporin as a model. J Neurosci Methods 103:83–90.
Matsushita T, Elliger S, Elliger C, Podsakoff G, Villarreal L, Kurtzman GJ, Iwaki Y, Colosi P (1998) Adeno-associated virus vectors can be efficiently produced without helper virus. Gene Ther 5:938–945.
Mohajeri MH, Figlewicz DA, Bohn MC (1999) Intramuscular grafts of myoblasts genetically modified to secrete glial cell line-derived neurotrophic factor prevent motoneuron loss and disease progression in a mouse model of familial amyotrophic lateral sclerosis. Hum Gene Ther 10:1853–1866.
Mourelatos Z, Gonatas NK, Stieber A, Gurney ME, Dal Canto MC (1996) The Golgi apparatus of spinal cord motoneurons in transgenic mice expressing mutant Cu, Zn superoxide dismutase becomes fragmented in early, preclinical stages of the disease. Proc Natl Acad Sci USA 93:5472–5477.
Oppenheim RW, Houenou LJ, Johnson JE, Lin LF, Li L, Lo AC, Newsome AL, Prevette DM, Wang S (1995) Developing motoneurons rescued from programmed and axotomy-induced cell death by GDNF. Nature 373:344–346.
Sagot Y, Tan SA, Hammang JP, Aebischer P, Kato AC (1996) GDNF slows loss of motoneurons but not axonal degeneration or premature death of pmn/pmn mice. J Neurosci 16:2335–2341.
Shibata N, Hirano A, Kobayashi M, Dal Canto MC, Gurney ME, Komori T, Umahara T, Asayama K (1998) Presence of Cu/Zn superoxide dismutase (SOD) immunoreactivity in neuronal hyaline inclusions in spinal cords from mice carrying a transgene for Gly93Ala mutant human Cu/Zn SOD. Acta Neuropathol 95:136–142.
Suzuki H, Hase A, Miyata Y, Arahata K, Akazawa C (1998) Prominent expression of glial cell line-derived neurotrophic factor in human skeletal muscle. J Comp Neurol 402:303–312.
Tsang YM, Chiong F, Kuznetsov D, Kasarskis E, Geula C (2000) Motoneurons are rich in non-phosphorylated neurofilaments: cross-species comparison and alterations in ALS. Brain Res 861:45–58.
Tu PH, Raju P, Robinson KA, Gurney ME, Trojanowski JQ, Lee VM (1996) Transgenic mice carrying a human mutant superoxide dismutase transgene develop neuronal cytoskeletal pathology resembling human amyotrophic lateral sclerosis lesions. Proc Natl Acad Sci USA 93:3155–3160.
Wang B, Li J, Xiao X (2000) Adeno-associated virus vector carrying human minidystrophin genes effectively ameliorates muscular dystrophy in mdx mouse model. Proc Natl Acad Sci USA 97:13714–13719.
Wang L, Muramatsu S, Lu Y, Ikeguchi K, Fujimoto K, Okada T, Mizukami H, Hanazono Y, Kume A, Urano F, Ichinose H, Nagatsu T, Nakano I, Ozawa K (2002) Delayed delivery of AAV-GDNF prevents nigral neurodegeneration and promotes functional recovery in a rat model of Parkinson's disease. Gene Ther 9:381–389.
Warita H, Itoyama Y, Abe K (1999) Selective impairment of fast anterograde axonal transport in the peripheral nerves of asymptomatic transgenic mice with a G93A mutant SOD1 gene. Brain Res 819:120–131.
Williamson TL, Cleveland DW (1999) Slowing of axonal transport is a very early event in the toxicity of ALS-linked SOD1 mutants to motoneurons. Nat Neurosci 2:50–56.
Wong PC, Pardo CA, Borchelt DR, Lee MK, Copeland NG, Jenkins NA, Sisodia SS, Cleveland DW, Price DL (1995) An adverse property of a familial ALS-linked SOD1 mutation causes motoneuron disease characterized by vacuolar degeneration of mitochondria. Neuron 14:1105–1116.
Xiao X, Li J, Samulski RJ (1996) Efficient long-term gene transfer into muscle tissue of immunocompetent mice by adeno-associated virus vector. J Virol 70:8098–8108.
Yamamoto M, Sobue G, Yamamoto K, Terao S, Mitsuma T (1996) Expression of glial cell line-derived growth factor mRNA in the spinal cord and muscle in amyotrophic lateral sclerosis. Neurosci Lett 204:117–120.
Yan Q, Matheson C, Lopez OT (1995) In vivo neurotrophic effects of GDNF on neonatal and adult facial motoneurons. Nature 373:341–344.

[CANCER RESEARCH 62, 2019–2023, April 1, 2002]

Soluble FLT-1 Expression Suppresses Carcinomatous Ascites in Nude Mice Bearing Ovarian Cancer[1]

Yoko Hasumi, Hiroaki Mizukami, Masashi Urabe, Takahiro Kohno, Koichi Takeuchi, Akihiro Kume, Mikio Momoeda, Hiroyuki Yoshikawa, Takashi Tsuruo, Masabumi Shibuya, Yuji Taketani, and Keiya Ozawa[2]

Division of Genetic Therapeutics [Y. H., H. M., M. U., T. K., A. K., K. O.] and Department of Anatomy, Jichi Medical School [K. T.], Tochigi 329-0498, and Department of Obstetrics and Gynecology, Faculty of Medicine 113-0033 [Y. H., M. M., H. Y., Y. T.], Institute of Molecular and Cellular Biosciences 113-0032 [T. T.], and Department of Genetics, Institute of Medical Science, University of Tokyo, Tokyo 108-8639 [M. S.], Japan

ABSTRACT

Vascular endothelial growth factor (VEGF), a bifunctional protein enhancing vascular permeability and stimulating endothelial growth, is thought to be responsible for fluid accumulation and angiogenesis in ascites tumors. To investigate the effects of stable expression of the soluble form of Flt-1 VEGF receptor (sFlt-1), a known endogenous inhibitor of VEGF, on the malignant ascites tumors, we cotransduced RMG-1 human ovarian cancer cells with adeno-associated virus vectors carrying the sFlt-1 cDNA and *Neo* gene or *Neo* gene alone and isolated both the sFlt-1-expressing clone and the Neo-expressing clone. *In vitro* growth characteristics were essentially the same. As expected, conditioned medium collected from the sFlt-1-expressing cells significantly inhibited the human umbilical vein endothelial cell proliferation in the presence of recombinant VEGF. Expression of sFlt-1 significantly suppressed RMG-1 cell-induced angiogenesis *in vivo* in the mouse dorsal air sac assay model. We then inoculated sFlt-1- or Neo alone-expressing cells i.p. into female BALB/c nude mice. The average volume of ascites fluid, number of leaked RBCs, and number of cancer cells were significantly lower in mice injected with sFlt-1-expressing cells than in the controls. Survival time was significantly prolonged in mice injected with sFlt-1-expressing cells. These results suggest that inhibition of VEGF activity by sFlt-1 expression may provide a means to control carcinomatous ascites and angiogenesis of malignant ascites tumors.

INTRODUCTION

More than half of all patients with ovarian cancer are not diagnosed until the advanced stages of the disease (1). One common pathway of tumor progression in ovarian carcinoma is peritoneal dissemination, and a progressive accumulation of ascites is frequent with or without malignant tumor cells. Both tumor size and the accumulation of ascites are inversely associated with survival (2, 3).

Tumor angiogenesis is critical for supporting the rapid growth of solid tumors (4) and is thought to be associated with the accumulation of malignant ascites. It was shown that marked peritoneal neovascularization accompanied some ascites tumors and that an angiogenesis inhibitor significantly reduced the accumulation of ascites after the inhibition of vessel proliferation (5, 6). Also, hyperpermeability of the microvessels lining the peritoneal cavity is considered to be essentially responsible for the accumulation of malignant ascites based on clinical (7, 8) and experimental observations (9–11). The hyperpermeability of microvessels associated with tumors has been shown to be mediated by a variety of factors including inflammatory mediators such as prostaglandin (12), leukokinins (13), bradykinin (14–16), histamine (17), and cytokines (18, 19). Among others, VEGF,[3] a bifunctional cytokine enhancing vascular permeability and stimulating endothelial growth, is thought to be responsible for fluid accumulation and angiogenesis in ascites tumors (20). VEGF exerts its functions by interacting with two different high affinity tyrosine kinase receptors, Flt-1 and/or KDR/Flk-1, which are selectively expressed in vascular endothelia (21).

It has been reported recently that human epithelial ovarian carcinomas overexpress VEGF with elevated serum VEGF levels being correlated with decreased survival (22). Given its potential role in promoting tumor angiogenesis, metastasis, and fluid accumulation, VEGF is an attractive target for therapeutic intervention. One strategy to block tumor angiogenesis and elevated vascular permeability is to perfuse the vasculature with a truncated sFlt-1. sFlt-1 is a known endogenously expressed selective inhibitor of VEGF. It is an alternatively spliced version of the Flt-1 VEGF receptor (23). The splicing alteration results in retention of an intron within the mRNA that is translated to the first in-frame stop codon. This alternatively spliced form of the Flt-1 protein retains six of seven NH_2-terminal extracellular immunoglobulin-like domains fused to the unique intron-encoded 31-amino acid residue COOH-terminal sequence but is devoid of the membrane proximal immunoglobulin-like domain, the membrane-spanning polypeptide, and the entire intracellular tyrosine kinase-containing region. The product, sFlt-1, binds to VEGF with the same affinity as and an equivalent specificity to the full-length receptor and forms a receptor-ligand complex. sFlt-1 is expressed by vascular endothelial cells and can inhibit their mitogenic response to VEGF in culture by sequestering VEGF. In addition, it interacts with the VEGF receptors in a dominant-negative fashion by heterodimerizing with the extracellular ligand-binding region of the membrane spanning Flt-1 (23) and KDR/Flk-1 (24) VEGF receptors, thereby blocking the activation of downstream signal transduction.

Given these properties of sFlt-1, it is of interest to see whether tumor cells engineered to express sFlt-1 exhibit diminished biological potentiality as tumors. In this study, we cotransduced RMG-1 human ovarian cancer cells with AAV vectors carrying sFlt-1 cDNA and the *Neo* gene, and isolated clones expressing sFlt-1. Here we demonstrated that an enhanced expression of sFlt-1 resulted in diminished endothelial cell-proliferating activity *in vitro* and suppression of angiogenesis *in vivo*. In addition, nude mice bearing the sFlt-1-expressing cancer cells exhibited a reduced accumulation of carcinomatous ascites and extended survival.

MATERIALS AND METHODS

Cell Lines. The 293 human embryonic kidney cell line (25) was maintained in DMEM-F12 plus 10% FBS, 2 mM glutamine, and 1% penicillin/streptomycin. RMG-1 human ovarian carcinoma cell line (26) was a gift from

Received 2/5/01; accepted 1/29/02.

The costs of publication of this article were defrayed in part by the payment of page charges. This article must therefore be hereby marked *advertisement* in accordance with 18 U.S.C. Section 1734 solely to indicate this fact.

[1] Supported in part by grants from the Ministry of Health, Labor and Welfare of Japan, grants-in-aid for Scientific Research from the Ministry of Education, Culture, Sports, Science and Technology, Japan, a grant-in-aid of the Japan Medical Association, and a grant from Takeda Science Foundation.

[2] To whom requests for reprints should be addressed, at Division of Genetic Therapeutics, Center for Molecular Medicine, Jichi Medical School, 3311-1 Yakushiji, Minamikawachi, Tochigi, 329-0498 Japan.

[3] The abbreviations used are: VEGF, vascular endothelial growth factor; sFlt-1, soluble form of the Flt-1 VEGF receptor; AAV, adeno-associated virus; FBS, fetal bovine serum; HUVEC, human umbilical vein endothelial cell.